

NAVAL POSTGRADUATE SCHOOL

Monterey, California

19971124 030

DTIC QUALITY INSPECTED 2



DTIC QUALITY INSPECTED 2

THESIS

**OPTIMUM CODES FOR FFH/BFSK RECEIVERS WITH
SELF-NORMALIZATION COMBINING AND HARD
DECISION DECODING IN FADING CHANNELS**

by

Xenofon Nikolakopoulos

March, 1997

Thesis Advisor:
Co-Advisor:

Tri T. Ha
R. Clark Robertson

Approved for public release; distribution is unlimited.

REPORT DOCUMENTATION PAGE			Form Approved OMB No. 0704-0188	
Public reporting burden for this collection of information is estimated to average 1 hour per response, including the time for reviewing instruction, searching existing data sources, gathering and maintaining the data needed, and completing and reviewing the collection of information. Send comments regarding this burden estimate or any other aspect of this collection of information, including suggestions for reducing this burden, to Washington headquarters Services, Directorate for Information Operations and Reports, 1215 Jefferson Davis Highway, Suite 1204, Arlington, VA 22202-4302, and to the Office of Management and Budget, Paperwork Reduction Project (0704-0188) Washington DC 20503.				
1. AGENCY USE ONLY (Leave blank)		2. REPORT DATE March 1997		3. REPORT TYPE AND DATES COVERED Master's Thesis
4. TITLE AND SUBTITLE OPTIMUM CODES FOR FFH/BFSK RECEIVERS WITH SELF-NORMALIZATION COMBINING AND HARD DECISION DECODING IN FADING CHANNELS			5. FUNDING NUMBERS	
6. AUTHOR(S) Nikolakopoulos, Xenofon				
7. PERFORMING ORGANIZATION NAME(S) AND ADDRESS(ES) Naval Postgraduate School Monterey, CA 93943-5000			8. PERFORMING ORGANIZATION REPORT NUMBER	
9. SPONSORING / MONITORING AGENCY NAME(S) AND ADDRESS(ES)			10. SPONSORING / MONITORING AGENCY REPORT NUMBER	
11. SUPPLEMENTARY NOTES The views expressed in this thesis are those of the author and do not reflect the official policy or position of the Department of Defense or the U.S. Government.				
12a. DISTRIBUTION / AVAILABILITY STATEMENT Approved for public release; distribution unlimited.			12b. DISTRIBUTION CODE	
13. ABSTRACT (<i>maximum 200 words</i>) <p>The application of forward error correction coding to a fast frequency-hopped binary frequency-shift keying (FFH/BFSK) noncoherent receiver with self-normalization combining under broadband and partial-band jamming is discussed in this thesis.</p> <p>The performance of the receiver is examined when data are encoded using Reed-Solomon codes, convolutional codes, and concatenated Reed-Solomon and convolutional codes, all with hard decision decoding. The effects of the transmission channel is considered, and results are derived for a Rayleigh fading channel and Ricean fading channels with several different ratios of direct-to-diffuse signal power. Only frequency nonselective, slowly fading channels are considered.</p> <p>The combination of diversity and forward error correction coding is found to improve the performance of the receiver in the presence of both broadband and partial-band jamming and optimum codes for each coding scheme are also discussed.</p>				
14. SUBJECT TERMS Fast frequency-hopping , self-normalization, Reed-Solomon coding, convolutional coding, concatenated coding			15. NUMBER OF PAGES 80	
			16. PRICE CODE	
17. SECURITY CLASSIFICATION OF REPORT Unclassified	18. SECURITY CLASSIFICATION OF THIS PAGE Unclassified	19. SECURITY CLASSIFICATION OF ABSTRACT Unclassified	20. LIMITATION OF ABSTRACT UL	

NSN 7540-01-280-5500

Standard Form 298 (Rev. 2-89)
Prescribed by ANSI Std. Z39-18

Approved for public release; distribution is unlimited

**OPTIMUM CODES FOR FFH/BFSK RECEIVERS WITH SELF-NORMALIZATION
COMBINING AND HARD DECISION DECODING IN FADING CHANNELS**

Xenofon Nikolakopoulos
Lieutenant, Hellenic Navy
B.S.E.E, Hellenic Naval Academy, 1988

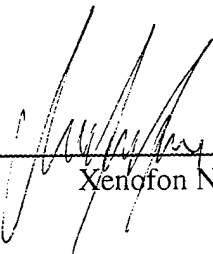
Submitted in partial fulfillment of the
requirements for the degree of

MASTER OF SCIENCE IN ELECTRICAL ENGINEERING

from the

**NAVAL POSTGRADUATE SCHOOL
March 1997**

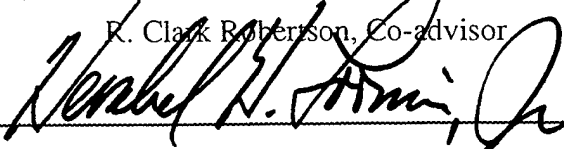
Author: _____


Xenofon Nikolakopoulos

Approved by: _____


Tri T. Ha, Thesis Advisor


R. Clark Robertson, Co-advisor


Herschel H. Loomis, Jr., Chairman
Department of Electrical and Computer Engineering

ABSTRACT

The application of forward error correction coding to a fast frequency-hopped binary frequency-shift keying (FFH/BFSK) noncoherent receiver with self-normalization combining under broadband and partial-band jamming is discussed in this thesis.

The performance of the receiver is examined when data are encoded using Reed-Solomon codes, convolutional codes, and concatenated Reed-Solomon and convolutional codes, all with hard decision decoding. The effects of the transmission channel is considered, and results are derived for a Rayleigh fading channel and Ricean fading channels with several different ratios of direct-to-diffuse signal power. Only frequency nonselective, slowly fading channels are considered.

The combination of diversity and forward error correction coding is found to improve the performance of the receiver in the presence of both broadband and partial-band jamming and optimum codes for each coding scheme are also discussed.

TABLE OF CONTENTS

I. INTRODUCTION	1
A. BACKGROUND	1
B. OBJECTIVE	5
II. PERFORMANCE ANALYSIS OF FAST FREQUENCY-HOPPED BFSK WITH SELF-NORMALIZATION COMBINING IN A FADING CHANNEL WITH PARTIAL-BAND INTERFERENCE AND WITHOUT CODING	7
A. ANALYSIS	9
B. PROBABILITY OF BIT ERROR	11
III. PERFORMANCE ANALYSIS OF FAST FREQUENCY-HOPPED BFSK WITH SELF-NORMALIZATION COMBINING IN A FADING CHANNEL WITH PARTIAL-BAND INTERFERENCE AND WITH REED-SOLOMON CODING	13
IV. PERFORMANCE ANALYSIS OF FAST FREQUENCY-HOPPED BFSK WITH SELF-NORMALIZATION COMBINING IN A FADING CHANNEL WITH PARTIAL-BAND INTERFERENCE AND WITH CONVOLUTIONAL CODING	17
V. PERFORMANCE ANALYSIS OF FAST FREQUENCY-HOPPED BFSK WITH SELF-NORMALIZATION COMBINING IN A FADING CHANNEL WITH PARTIAL-BAND INTERFERENCE AND WITH CONCATENATED CODING	21
VI. NUMERICAL RESULTS	23
A. REED-SOLOMON CODING	23
B. CONVOLUTIONAL CODING	25
C. CONCATENATED CODING	26
VII. CONCLUSIONS	29

REFERENCES	69
INITIAL DISTRIBUTION LIST	71

I. INTRODUCTION

A. BACKGROUND

Digital communication systems nowadays are taking the place of the previous analog systems because the tremendous evolution in technological achievements makes it not only feasible but necessary. At the same time, the increase in the demands for more reliable and complex systems pushes technology to its limits. Digital signals have many advantages over analog signals: they suffer less from distortion and interference and can easily be reproduced (regenerated) [Ref. 1]; using digital signals, higher data rates can be achieved over a bandwidth limited channel; and forward error correction coding techniques can be applied.

Military applications as well as many commercial applications in wireless communications are leading research to areas that are new and more efficient. One of these areas is the study of the so called spread spectrum (SS) signals. Spread spectrum signals are used mainly in communications, but there are other applications of spread spectrum, such as to obtain accurate range and velocity measurements in radar and navigation [Ref. 2].

By definition, spread spectrum modulation uses a transmission bandwidth many times greater than the information bandwidth. One consequence of this wide bandwidth is that, for some types of spread spectrum signals, the signal spectrum cannot be distinguished from the background noise (low-probability-of-detection or LPD signals) [Ref. 3]. One important advantage of spread spectrum signals is that it makes possible to overcome the effects of interference whether it is intentional (i.e., jamming) or unintentional (i.e., from other users of the same channel or due to multipath propagation). Message privacy from unintended listeners is achieved due to the pseudo-random pattern imposed on the transmitted signal (low-probability-of-intercept or LPI signals) [Ref. 2].

Two types of modulation are widely used in digital communication systems with spread spectrum signals: phase-shift keying (PSK) and frequency-shift keying (FSK).

Modern jammers have the capability to copy and reproduce signals that are emitted and in this way to confuse the receiver. More sophisticated transmitters can overcome this by introducing a pseudo-random or pseudo-noise (PN) sequence in the transmitted signal. The notion of pseudo-randomness is that the sequence appears random but can be reproduced in the receiver using deterministic means. Since this pattern is known only to the receiver and not to the jammer, we expect the system to be more difficult to jam. When a PN sequence is used with PSK modulation so that the phase of the signal is shifted in a pseudo-random way, the resulting signal is called a direct sequence (DS) spread spectrum signal. When it is difficult to maintain phase coherence, noncoherent FSK is used and instead of randomly shifting the phase, the carrier frequency of the signal is selected according to a pseudo-random pattern. The resulting signal is called a frequency-hopped spread spectrum signal. In this case, the available channel bandwidth is divided into frequency slots and the transmitter changes (hops) its RF carrier frequency in a pseudo-random way according to the output of a PN generator from one slot to another. The most commonly used scheme in this category is frequency-hopped noncoherent M-ary FSK (FH/MFSK). When one or more symbols is transmitted for a single hop, the system is referred to as slow frequency hopped (SFH). On the other hand, when one symbol is transmitted on multiple hops, the system is referred to as fast frequency-hopped (FFH) [Ref. 4]. Other possible SS systems are time hopping (TH) or some hybrid combinations such as DS/FH. DS and FH are currently the most commonly used spread spectrum signal types.

An important aspect in a communication system is the transmission channel. The classical additive white Gaussian channel (AWGN) does not model all the existing channel types. For many military and commercial communication systems, the transmission channel is more complex as the physical characteristics of the media are continuously changing. These channels have randomly time-variant impulse responses; and as a result, if the same signal is transmitted in two different time intervals the channel will affect the signal differently. Especially in the presence of multiple propagation paths with time-variant propagation delays and attenuation factors, the resulting signal amplitude through the

different paths is sometimes large and other times small. These amplitude variations are called signal fading, and the corresponding channels are called fading multipath channels. In many cases the signaling interval is smaller than the coherence time of the channel, and the channel attenuation can be considered to be fixed during the signaling interval. These type of channels are defined as slowly fading channels. When the coherence bandwidth of the channel is smaller than the bandwidth of the transmitted signal, the signal is severely distorted by the channel. The channel in this case is characterized as frequency-selective in contrast to a frequency-nonselective channel where the coherence bandwidth of the channel is large compared to the bandwidth of the transmitted signal [Ref. 2]. In this thesis, only slowly fading, frequency-nonselective channels are considered. A common fading multipath channel in communications is modeled as a Rayleigh fading channel. In some other applications, like satellite communications, there is a direct path between the transmitter and the receiver that is added to the multipath components. This type of channel is modeled as Ricean fading channel.

The main problem when transmitting over a fading channel is that in order to achieve good performance (low probability of symbol error) the transmitter has to use a large amount of power. In most cases this is neither possible nor desirable. One way to overcome this problem is the use of redundancy that can be provided either by diversity techniques [Ref. 2] or by the use of forward error correction coding [Ref. 3].

When the same information signal is transmitted several times over independently fading channels it is unlikely that all the components will fade simultaneously at the receiver. This is the basic concept of diversity techniques. There are several methods used in practice, but the most widely used are time-diversity, frequency diversity, and space diversity. In time diversity the same information signal is transmitted in different time slots where the separation between time slots equals or exceeds the coherence time of the channel. When the same information signal is transmitted on different carriers and the separation between successive carriers equals or exceeds the coherence bandwidth of the channel, the technique is referred as frequency diversity [Ref. 2]. In space or antenna diversity, multiple receiving (and possibly multiple transmitting) antennas are spaced with

a separation of least ten wavelengths. In this way the received signals in the spaced antennas fade independently [Ref. 2] , [Ref. 5].

As diversity is a sort of repetition coding, it is reasonable to expect that the use of forward error correcting coding (FEC) will further improve the performance of a system. Actually the use of FEC can improve the performance not only of fixed amplitude and phase channels but of fading channels as well [Ref. 3]. Theoretically, if the information data rate is less than the channel capacity, it is possible to achieve as small a probability of symbol error as desired with the use of the proper coding techniques. The critical limitation is that the resulting system may be too expensive to implement. Building systems that are both cost effective and efficient is a research area of great interest.

The two main types of codes used in practice are block codes and tree codes. In block codes, k information symbols are mapped into an n symbol block that depends only upon the specific k symbols and no others. The encoder is characterized as memoryless. On the other hand, the encoder for a tree code maps k information symbols into an n symbol sequence that depends on the current k input symbols as well as on v preceding input symbols. The encoder in this case has memory [Ref. 6]. On the receiver end, the decoder is a device that estimates the most likely transmitted code word based on the received one. For the decoding of block codes, procedures are based on elementary code structure or the algebraic structure of certain codes (i.e., Reed-Solomon decoding). Decoding of tree codes may be achieved using the Viterbi algorithm (maximum-likelihood decoding) [Ref. 7], sequential decoding algorithms, or threshold decoding. If binary quantization is used at the output of the decoder, it is referred to as hard decision decoding in contrast to soft decision decoding when m -bit quantization is used (with $m > 2$).

When very long codes with large error correction capability are desired, multiple levels of coding may be used. This is referred to as concatenated coding. In the most preferred scheme, two levels of coding are used. One of the codes is usually nonbinary and is called the outer code and the other is binary and is called the inner code. Although any kind of codes may be used as inner and outer codes in combination of hard or soft

decision decoding, most of the time Reed-Solomon codes are preferred as outer codes. Systems with Viterbi-decoded convolutional inner codes with relatively short constraint length (<10) were shown in [Ref. 8] to have good performance.

B. OBJECTIVE

In this thesis, the coded performance of a fast frequency-hopped binary frequency shift keying (FFH/BFSK) non-coherent receiver with self-normalization combining is examined. Self-normalization combining is a technique used to minimize performance degradation due to partial-band interference. The uncoded performance of the receiver has been previously examined [Ref. 9] and [Ref. 10]. The effects of the application of forward error correction coding in combination with frequency diversity for the specific receiver is here investigated.

Three different types of codes with hard decision decoding are evaluated to find the optimum coding scheme. First of all, Reed-Solomon (RS) codes of different code rates are examined in Chapter III. The application of Reed-Solomon codes in frequency-hop communications has been previously studied [Ref. 11]. The performance of convolutional codes of various code rates and constraint lengths and convolutional codes concatenated with RS codes is evaluated in Chapter IV and Chapter V, respectively. The coded performance is compared with the uncoded for the optimum codes found in each case.

Results are obtained for partial-band and broadband interference and for several types of transmission channels: a Rayleigh fading channel and Ricean fading channels with several different ratios of direct-to-diffuse signal power.

II. PERFORMANCE ANALYSIS OF FAST FREQUENCY-HOPPED BFSK WITH SELF-NORMALIZATION COMBINING IN A FADING CHANNEL WITH PARTIAL-BAND INTERFERENCE AND WITHOUT CODING

The performance of a fast frequency-hopped BFSK receiver with self-normalization combining in a fading channel with partial-band interference has been previously examined [Ref. 9]. The transmitter is assumed to send L hops per data bit. At the receiver (Fig. 1) the dehopped signals are demodulated by a bandpass filter with equivalent noise bandwidth of B Hz followed by a quadratic detector. Self-normalization combining is used to nonlinearly combine the outputs of the quadratic detectors of the two branches of the BFSK demodulator to form the L diversity signals which are then combined to obtain the decision statistics [Ref. 9].

The channel for each hop is modeled as a frequency-nonselective, slowly fading Ricean process. This means that we consider the signal bandwidth to be much smaller than the coherence bandwidth of the channel and the hop rate much greater than the Doppler spread of the channel [Ref. 2]. In this case the dehopped signal can be modeled as the sum of a nonfaded (direct) and a Rayleigh-faded (diffuse) component.

Interference is considered to be both partial-band (caused by a jammer or any other source of narrowband interference) and wideband interference (i.e., thermal noise). Partial-band interference is modeled as additive Gaussian noise with power spectral density

$$N_{I_\gamma} = \gamma^{-1} \frac{N_I}{2} \quad (1)$$

where γ is the fraction of the bandwidth being jammed and

$N_I/2$ is the average interference noise power spectral density over the entire bandwidth.

Wideband interference is modeled as additive white Gaussian noise with noise power spectral density $N_0/2$.

The noise power for each hop k of a signal is

$$\sigma_{\kappa}^2 = (\gamma^{-1} N_I + N_0) B \quad (2)$$

with probability γ when interference is present and

$$\sigma_{\kappa}^2 = N_0 B$$

with probability $1-\gamma$ when interference is not present.

For a bit interval duration of T_b seconds, the bit rate is $R_b = 1/T_b$. The duration of the hop interval is $T_h = T_b/L$ for L^{th} order diversity, and the hop rate is $R_h = 1/T_h = L R_b$. If S is the average signal power, then

$$S = a^2 + 2\sigma^2 \quad (3)$$

where a^2 is the average power of the direct component of the signal and $2\sigma^2$ is the average power of the diffuse component of the signal.

In this case the average energy per hop is $E_h = S T_h$ and the average energy per bit is $E_b = L E_h$. The signal power-to-noise power ratio is

$$\frac{S}{\sigma_{\kappa}^2} = \frac{E_h \cdot R_h}{N_T \cdot B} = \frac{E_b \cdot R_b}{L \cdot N_T \cdot B} \quad (4)$$

where $N_T/2$ is the power spectral density of the total noise power.

Since there is no other modulation scheme, the minimum equivalent noise bandwidth of the signal is equal to the hop rate we can use $B=R_h$ [Ref. 9], and (4) can be rewritten as:

$$\frac{S}{\sigma_k^2} = \frac{E_h}{N_T} = \frac{E_b}{L \cdot N_T} \quad (5)$$

A. ANALYSIS

The probability density function $f_{X_{1k}}$ of the random variable X_{1k} that models the output of the quadratic detector assuming that the signal is present in branch 1 and the probability density function $f_{X_{2k}}$ of the random variable X_{2k} that models the output of branch 2 that contains no signal of the BFSK demodulator are given in [Ref. 9] as:

$$f_{X_{1k}}(x_{1k}) = \frac{1}{2 \cdot (\sigma_k^2 + 2\sigma^2)} \cdot e^{-\left(\frac{1}{2} \frac{x_{1k} + 2\sigma^2}{\sigma_k^2 + 2\sigma^2}\right)} \cdot I_0\left(\frac{\alpha \sqrt{2 \cdot x_{1k}}}{\sigma_k^2 + 2\sigma^2}\right) \cdot u(x_{1k}) \quad (6)$$

$$f_{X_{2k}}(x_{2k}) = \frac{1}{2 \cdot \sigma_k^2} \cdot e^{-\left(\frac{x_{2k}}{\sigma_k^2}\right)} \cdot u(x_{2k}) \quad (7)$$

where $I_0(.)$ is the modified Bessel function of zero order and $u(.)$ is the unit step function.

The normalized random variable Z_{ik} , $i=1,2$ is given by

$$Z_{ik} = \frac{X_{ik}}{X_{1k} + X_{2k}} \quad (8)$$

and the probability density function of Z_{ik} is [Ref. 9]:

$$f_{Z_{1k}}(z_{1k}) = \frac{\rho_k \cdot z_{1k} + (1 + \xi_k) \cdot [1 + \xi_k \cdot (1 - z_{1k})]}{[1 + \xi_k \cdot (1 - z_{1k})]^3} \cdot e^{\left(\frac{-\rho_k \cdot (1 - z_k)}{1 + \xi_k \cdot (1 - z_k)}\right)} \quad (9)$$

for $0 \leq z_{1k} \leq 1$

where $\rho_k = a^2/\sigma_k^2$ is the signal-to-noise ratio of the direct component of hop k of a bit and $\xi_k = 2\sigma^2/\sigma_k^2$ is the signal-to-noise ratio of the diffuse component of hop k of a bit.

If we define as $\lambda = \rho_k/\xi_k = a^2/2\sigma^2$ the ratio of the direct-to-diffuse power components, then (8) can be rewritten as a function of λ as:

$$f_{Z_{1k}}(z_{1k}) = \frac{\xi_k \cdot \lambda \cdot z_{1k} + (1 + \xi_k) \cdot [1 + \xi_k \cdot (1 - z_{1k})]}{[1 + \xi_k \cdot (1 - z_{1k})]^3} \cdot e^{\left(\frac{-\xi_k \cdot \lambda \cdot (1 - z_k)}{1 + \xi_k \cdot (1 - z_k)}\right)} \quad (10)$$

for $0 \leq z_{1k} \leq 1$

Since $\rho_k = a^2/\sigma_k^2$ and $\xi_k = 2\sigma^2/\sigma_k^2$, then from (5):

$$\rho_k + \xi_k = \frac{a^2 + 2\sigma^2}{\sigma_k^2} = \frac{S}{\sigma_k^2} = \frac{E_b}{L \cdot N_T} \quad (11)$$

This implies:

$$\xi_{\kappa} \cdot \left(1 + \frac{\rho_{\kappa}}{\xi_{\kappa}}\right) = \frac{E_b}{L \cdot N_T} \Rightarrow \xi_{\kappa} \cdot (1 + \lambda) = \frac{E_b}{L \cdot N_T} \quad (12)$$

and in turn:

$$\xi_{\kappa} = \frac{1}{1 + \lambda} \frac{E_b}{LN_T} = \frac{1}{(1 + \lambda)L} \frac{E_b/N_0}{1 + \frac{E_b/N_0}{E_b/N_I} \gamma^{-1}} \quad (13)$$

B. PROBABILITY OF BIT ERROR

The conditional probability density function for Z_I given that i hops of a bit have interference has been derived in [Ref. 9] as:

$$f_{Z_I}(Z_I/i) = \left[f_{Z_{k1}}^{(1)}(Z_{1k}) \right]^{\otimes i} \otimes \left[f_{Z_{k1}}^{(2)}(Z_{1k}) \right]^{\otimes (L-i)} \quad (14)$$

where $f_{Z_{k1}}^{(1)}(Z_{1k})$ is the probability density function of Z_{1k} assuming that hop k of a bit has interference, $f_{Z_{k1}}^{(2)}(Z_{1k})$ is the probability density function of Z_{1k} assuming that hop k of a bit has no interference, and $\otimes i$ represents an i -fold convolution.

The conditional bit error probability given that i hops of a bit have interference is derived in [Ref. 9] as:

$$P_b(i) = \int_0^{L/2} f_{Z_I}(Z_I/i) dz_1 \quad (15)$$

and the uncoded bit error probability for the receiver is

$$P_b = \sum_{i=0}^L \binom{L}{i} \cdot \gamma^i \cdot (1-\gamma)^{L-i} \cdot P_b(i) \quad (16)$$

In the general case $f_{zi}(z/i)$ and $P_b(i)$ must each be evaluated numerically.

In general, self-normalization combining with diversity is insufficient to reduce the probability of bit error to acceptable levels. Generally, some sort of forward error correction coding is also necessary. In the next chapter, the performance of the fast frequency-hopped BFSK receiver with self-normalization combining and Reed-Solomon coding is examined. Convolutional and concatenated codes are examined in later chapters.

III. PERFORMANCE ANALYSIS OF FAST FREQUENCY-HOPPED BFSK WITH SELF-NORMALIZATION COMBINING IN A FADING CHANNEL WITH PARTIAL-BAND INTERFERENCE AND WITH REED-SOLOMON CODING

For the last thirty years, Reed-Solomon codes have played a very important role in numerous engineering designs and implementations. Applications of Reed-Solomon codes cover a large spectrum of areas from entertainment (i.e., compact disk players) to space exploration (i.e., the Voyager mission). In the development of digital communication systems and especially in spread spectrum systems, Reed-Solomon codes are a basic tool that provides performance improvement and thus more efficient and reliable systems [Ref. 11]. One advantage of Reed-Solomon codes is that they are a family of nonbinary codes. As such, they work well with modulation formats designed for power-limited channels such as MFSK.

The original construction of Reed-Solomon codes was through the use of finite field arithmetic, also referred to as Galois fields (GF). Two arithmetic operations, addition and multiplication, are defined on the elements of a finite field. The number q of elements in a finite field $GF(q)$ must be in the form p^m where p is a prime integer and m is a positive integer. In $GF(q)$ there is at least one element and $q-1$ nonzero elements.

If k information symbols i_0, i_1, \dots, i_{k-1} taken from $GF(q)$ are used to construct an information polynomial $I(x) = i_0 + i_1x + \dots + i_{k-1}x^{k-1}$, then a Reed-Solomon code word is formed by evaluating $I(x)$ at each of the q elements in $GF(q)$. Using all possible values, a complete set of q^k code words can be constructed to form a Reed-Solomon code. Since the sum of any two Reed-Solomon code words is also a code word, Reed-Solomon codes are linear codes. The number k of information symbols and the length $n=q$ characterize a Reed-Solomon code as an (n,k) code.

For Reed-Solomon codes with code words of length n symbols, each with k information symbols, the number of errors t that the code can correct and the minimum distance of the code d_{min} are given as [Ref. 2]:

$$k = 1, 3, \dots, n-2 \quad (17)$$

$$t = \frac{n-k}{2} \quad (18)$$

$$d_{min} = n - k + 1 \quad (19)$$

There are several other approaches to the construction of Reed-Solomon codes such as the GF Fourier transform approach, but the most popular nowadays is the generator polynomial approach [Ref. 11].

A code is said to be cyclic if any cyclic shift of a code word $c = c_0, c_1, \dots, c_{n-1}$, results in a code word (i.e., c_1, \dots, c_{n-1}, c_0). An (n,k) cyclic code can be represented in polynomial form ($\alpha(x) = c_0 + c_1x + \dots + c_{n-1}x^{n-1}$) and:

$$\alpha(x) = I(x)g(x) \quad (20)$$

where $I(x)$ is the information polynomial and $g(x) = g_0 + g_1x + \dots + g_{n-1}x^{n-1}$ is the generator polynomial.

Cyclic Reed-Solomon codes have length $n = q-1$, one less than the original construction. As an example, in GF(32) the cyclic Reed-Solomon code will have a length $n=31$. The generator polynomial approach in the construction of Reed-Solomon codes is used in this thesis.

The performance of a fast frequency-hopped BFSK receiver with self-normalization combining in a fading channel with partial band interference and with Reed-Solomon error correction coding is now examined.

In forward error correction coding, n coded symbols are transmitted for k information symbols. In order to maintain a fixed data rate,

$$n \cdot T_c = k \cdot T_b \Rightarrow R_c = \frac{R_b}{k/n} = \frac{R_b}{\tau} \quad (21)$$

where T_b is the bit duration,

T_c is the coded bit duration,

R_b is the bit rate,

R_c is the coded bit rate and

τ is the code rate k/n .

For the analysis that follows it is assumed that the transmitted power P as well as the bit rate R_b are fixed. In this case, E_b is also fixed since:

$$P = E_b \cdot R_b \quad (22)$$

So for variable code rate $\tau=k/n$, the coded bit energy E_c will vary for constant transmitted power since:

$$P = E_b \cdot R_b = E_c \cdot R_c \Rightarrow E_c = \tau \cdot E_b \quad (23)$$

The performance of this coding/modulation scheme with hard decision decoding is given analytically in [Ref. 2] as:

$$P_b = \frac{M}{2 \cdot (M-1)} \cdot \left[\frac{1}{n} \cdot \sum_{i=t+1}^n i \cdot \binom{n}{i} \cdot p_s^i \cdot (1-p_s)^{n-i} \right] \quad (24)$$

For the binary case with $M=2$ (20) is reduced to :

$$P_b = \frac{1}{n} \cdot \sum_{i=t+1}^n i \cdot \binom{n}{i} \cdot p_s^i \cdot (1-p_s)^{n-i} \quad (25)$$

where p_s is the uncoded bit error probability given by (16).

Using (23), the signal-to-noise ratio in the uncoded symbol error probability p_s given by (16) will be scaled by the code rate $r=k/n$.

The performance of the fast frequency-hopped BFSK receiver with self-normalization combining in a fading channel using convolutional codes is examined in the next chapter.

IV. PERFORMANCE ANALYSIS OF FAST FREQUENCY-HOPPED BFSK WITH SELF-NORMALIZATION COMBINING IN A FADING CHANNEL WITH PARTIAL-BAND INTERFERENCE AND WITH CONVOLUTIONAL CODING

The Reed-Solomon codes studied in the previous chapter are based on algebraic properties and consist of fixed length independent code words. Convolutional codes, studied in this chapter, are different because information symbols are coded based on the current data bits as well as on a number of preceding bits. Algebraic techniques used for error correction in block codes are not applicable in this case, and the maximum-likelihood decoding algorithm (Viterbi algorithm) is widely used instead. Convolutional codes have the advantages of combining relatively simple implementation and good coding gains.

A convolutional encoder for a rate k/n code can be implemented using k shift registers and n modulo-2 adders. Since the set of n coded bits is determined by the k information bits and $k(v-1)$ preceding bits, at least one of the k shift registers must have $v-1$ stages. A convolutional code is characterized by the code rate k/n and a parameter called the constraint length of the convolutional code. In some references the parameter v is referred to as the constraint length of the code. In other references, the constraint length is defined as the number of k -bit stages of the shift register [Ref. 2], or as the maximum number of coded bits that can be affected by a single information bit ($v' = nv$) [Ref. 13], or as the length of the shift register ($v_c = v-1$) [Ref. 6]. For the purposes of this thesis, the latter definition will be used.

To describe a convolutional code one can use the generator matrix. The generator matrix \mathbf{G} consists of the generator polynomials $g(x)$ that describe the connections between the shift register stages and the modulo-2 adders. The code word \mathbf{C} corresponding to any information vector \mathbf{I} is obtained by multiplying the information vector with the generator matrix [Ref. 6]:

$$\mathbf{C} = \mathbf{I}^T \mathbf{G} \quad (26)$$

As an example, for a rate 1/2 convolutional code the generator vectors are $\mathbf{g}_1 = [1\ 0\ 1\ 0\ 0\ \dots]$ and $\mathbf{g}_2 = [1\ 1\ 1\ 0\ 0\ \dots]$ with corresponding generator polynomials $g_1(x) = 1 + 0x + 1x^2$ and $g_2(x) = 1 + 1x + 1x^2$. The resulting code word in this case is $\mathbf{C} = [c_1(x)\ c_2(x)]$ with $c_1(x) = I(x)g_1(x)$ and $c_2(x) = I(x)g_2(x)$.

Another way to describe a convolutional encoder is as a finite-state machine with 2^v states, where v is the constraint length of the code. To better explain this, the example of a rate 1/2 convolutional code with constraint length of $v=2$ is used. The equivalent signal flow graph for the specific code is given in Fig. 2 where S_0, S_1, S_2 , and S_3 are the states of the finite-state machine [Ref. 6].

In this flow graph, each branch is labeled with D^w , N^{wl} , and L where w is the Hamming distance of the encoder output corresponding to the branch, wl is the weight of the input sequence of the branch, and L is the length of the branch. The Hamming distance is the number of coordinates in which two code words differ, and weight is the number of nonzero elements of a code word. The minimum distance between any two distinct code words is called the free distance d_f .

Using Mason's gain formula from the theory of signal flow graphs, the transfer function $T(D, L, N)$ can be obtained. The total information weight w_j of all paths of weight j can be calculated by differentiating the transfer function $T(D, L, N)$ with respect to N and setting $N=1$ [Ref. 6]:

$$\left. \frac{\partial T(D, L, N)}{\partial N} \right|_{N=1} = \sum_{j=0}^{\infty} w_j D^j \quad (27)$$

Using the Viterbi decoding algorithm and hard decision decoding, we have the probability that an incorrect path will be selected in [Ref. 2]:

$$P_j = \sum_{d=\frac{d_f+1}{2}}^{d_f} \binom{d_f}{d} p^d (1-p)^{d_f-d} \quad (28)$$

if d is odd, and

$$P_j = \sum_{d=\frac{d_f}{2}}^{d_f} \binom{d_f}{d} p^d (1-p)^{d_f-d} + \frac{1}{2} \binom{d_f}{\frac{d_f}{2}} p^{\frac{d_f}{2}} (1-p)^{\frac{d_f}{2}} \quad (29)$$

if d is even. In (28) and (29), p is the uncoded bit error probability of a fast frequency-hopped BFSK receiver with self-normalization combining in a fading channel with partial-band interference and is given by (16) for this thesis.

The union bound for the coded bit error probability is given in [Ref. 2] as:

$$P_b \leq \sum_{j=d_f}^{\infty} w_j P_j \quad (30)$$

where P_j is given by (28) and (29) and the weight structure w_j is obtained from (27). The weight structure is given in [Ref. 6] for codes of different rates and constraint lengths.

The assumption made in Chapter V, that the transmitted power as well as the bit rate are fixed, is made in this case too. So, using (23), the signal-to-noise ratio in the uncoded symbol error probability is scaled by the code rate $R=k/n$.

In the next chapter, the performance of the fast frequency-hopped BFSK receiver with self-normalization combining in a fading channel using concatenated codes is examined.

V. PERFORMANCE ANALYSIS OF FAST FREQUENCY-HOPPED BFSK WITH SELF-NORMALIZATION COMBINING IN A FADING CHANNEL WITH PARTIAL-BAND INTERFERENCE AND WITH CONCATENATED CODING

Concatenated coding with Reed-Solomon codes as outer codes and convolutional codes as inner codes are discussed in this chapter. The nonbinary outer code has a code rate $R_o = k_o/n_o$, and the binary inner code has a code rate $R_i = k_i/n_i$. The resulting code has a length of $n = n_o n_i$, k information bits with $k = k_o k_i$, and code rate $R = R_o R_i = k_o k_i / n_o n_i$. An encoding-decoding scheme for concatenated codes is shown in Fig. 3 where the combination of inner encoder, channel, and inner decoder is called the superchannel.

In the transmitter, the k information bits are grouped into k_o symbols each one consisting of k_i bits. Then the outer encoder encodes the k_o symbols into n_o symbols, each one consisting of k_i bits. Each of these symbols are further encoded by the inner encoder into a binary convolutional code of length n_i .

At the receiver, the inner decoder uses hard decision decoding to regroup the received bits into groups of n_i bits that correspond to a convolutional code word. After this decision, the inner decoder makes a decision on the k_i information bits (that form one symbol of the Reed-Solomon code) using the Viterbi decoding algorithm. In this way, the beginning of each Reed-Solomon code symbol is determined. Then the outer decoder makes a hard decision, correcting as many symbol errors as possible.

Since the inner decoder performs hard decision decoding for a binary convolutional code, the union bound for the coded bit channel transition probability is the one given in (30) as:

$$P_i \leq \sum_{j=d_f}^{\infty} w_j P_j$$

where P_j is given by (28) and (29) and the weight structure w_j is found in [Ref. 6] for codes of different rates and constraint lengths.

The symbol channel transition probability P_s at the input of the Reed-Solomon decoder is given as a function of P_i as

$$P_s \approx 1 - (1 - P_i)^m \quad (31)$$

where $2^m - 1 = n_o$ and n_o is the length of the Reed-Solomon code used as outer code.

The union bound for the bit error probability at the output of the outer (Reed-Solomon) decoder is given in [Ref. 2]-[Ref. 6] as

$$P_b \leq \frac{2^{m-1}}{2^m - 1} \sum_{j=t+1}^{n_o} \frac{j}{n} \binom{n_o}{j} P_s^j (1 - P_s)^{n_o-j} \quad (32)$$

where P_s is given by (31), and $t = \frac{n_o - k_o}{2}$ is the number of errors the Reed-Solomon code can correct.

Given that $2^m - 1 = n_o$ and $2^{m-1} = \frac{n_o + 1}{2}$, (32) can be rewritten as:

$$P_b \leq \frac{n_o + 1}{2n_o} \sum_{j=t+1}^{n_o} j \binom{n_o}{j} P_s^j (1 - P_s)^{n_o-j} \quad (33)$$

The assumption made in Chapter V that the transmitted power as well as the bit rate are fixed is made in this case too. So, using (23), the signal-to-noise ratio in the uncoded symbol error probability is scaled by the code rate $R = k_o k_i / n_o n_i$.

VI. NUMERICAL RESULTS

From the analysis performed in [Ref. 9] for the uncoded performance of fast frequency-hopped BFSK receiver with self-normalization combining in a fading channel with partial-band interference, it is clear that for a relatively large number of diversity levels ($L > 3$) worst case performance (assuming the same jammer power for both broadband and partial-band cases) corresponds to broadband interference (i.e., the whole bandwidth is jammed) or, equivalently, when all hops of a bit are jammed ($\gamma=1$ or $i=L$ respectively). This assumption has been made for the purposes of the numerical analysis of the coded performance of the system, and a diversity level of $L=4$ has been considered. The probability of bit error as a function of the bit energy-to-interference noise density ratio E_b/N_I has been examined for Reed-Solomon codes of length $n=7, 15$, and 31 , convolutional codes of rate $1/2$ and $1/3$, and concatenated codes with a convolutional code of rate $3/4$ and constraint length $v=8$ used as inner code and various length Reed-Solomon codes used as outer codes. The ratio of bit energy-to-thermal noise density E_b/N_0 is taken to be 13.35 dB in the first two cases and 18 dB in the study of concatenated codes. This value of E_b/N_0 corresponds to $P_b=10^{-5}$ when there is no fading and $L=1$ [Ref. 9].

The effect of the channel for a number of different fading cases is examined. Results are derived for a very strong ($a^2/2\sigma^2=100$), a strong ($a^2/2\sigma^2=20$), a relatively strong ($a^2/2\sigma^2=10$), and an average ($a^2/2\sigma^2=5$) direct signal as well as for a Rayleigh channel model ($a^2/2\sigma^2=0$).

A. REED-SOLOMON CODING

The performance of systems using Reed-Solomon codes of length $n=7$ for the different channel models is shown in Figs. 3-6. In all cases, if E_b/N_I exceeds a threshold of approximately 6 dB, then the code RS(7,5) has better performance than the others

(RS(7,1) and RS(7,3)). The performance is better in the presence of a direct signal and improves more as the direct signal becomes stronger

Similar results are obtained for codes of length $n=15$ as can be seen in Figs 7-9. For E_b/N_t greater than approximately 9 dB, the code (15,7) for the Rayleigh channel and (15,9) for the Ricean channels outperforms the other codes of the same length. The presence of the direct signal gives the opportunity to use a slightly higher rate code (15,9) than in the Rayleigh case. Based on the fact that in the absence of a direct component the two codes have almost the same performance (Fig. 7), we can argue that in all cases the (15,9) code gives the optimum performance compared with codes of the same length.

Among all codes with length $n=31$, for a Rayleigh channel model the (31,15) code has the best performance (Fig. 10). To achieve this improvement, the ratio E_b/N_t must exceed approximately 9 dB. In the presence of an increasingly strong direct signal, higher rate codes can be used (Figs. 11-12) to improve performance. For $a^2/2\sigma^2=5$, the (31,17) code is best; but as the direct signal becomes stronger, the (31,19) code is optimum. When we further increase the direct signal to $a^2/2\sigma^2=20$ (Fig. 13) and $a^2/2\sigma^2=100$ (Fig.14), there is no higher rate code that outperforms (31,19). This leads to the conclusion that the performance of the system is limited by a code rate of about 2/3.

For error correction codes it seems reasonable that the redundancy provided by the parity bits improves the performance of any system. This means that we expect that the fewer the information symbols used in a code word, the better the performance. This is not always the case. When the transmitted power and the bit rate are fixed, the bit energy is constant, but the coded bit energy increases as we increase the number of information symbols. This increase in coded bit energy can, in some circumstances, overcome the advantage that additional redundant bits provide, giving higher rate codes with better performance.

In Figs. 15-17, the performance of optimum codes of different lengths is compared with uncoded performance for the three different channel models. When E_b/N_t exceeds approximately 9-10 dB, the coded performance is much better than the uncoded. It is of note that with an increase in coded bit energy, longer codes outperform shorter

ones and the probability of bit error for a specific case ($a^2/2\sigma^2=10$) can reach $P_b=10^{-5}$ with $E_b/N_f=18$ dB using a (31,19) Reed-Solomon code.

In Figs. 18-19 the performance of optimum Reed-Solomon codes of length 7, 15, and 31 is examined in the presence of partial-band interference and compared with uncoded performance. As in the study of the uncoded case [Ref. 9], the smaller the fraction of the bandwidth being jammed, the better the performance of the system assuming identical jamming power. Results were derived for $\gamma=0.1$ and $\gamma=0.01$ in a Rayleigh channel (Fig. 18) and for $\gamma=0.1$ in a Ricean channel with $a^2/2\sigma^2=10$ (Fig. 19). As shown in Fig. 18, the performance of the system reaches its asymptotic limit for $E_b/N_f > 30$ dB no matter what fraction of the bandwidth is jammed and for all coded and uncoded cases.

B. CONVOLUTIONAL CODING

The performance of the system with convolutional codes of rates 1/2 and 1/3 and constraint lengths of $v=6$ and $n=7$ for three different channel models in broadband jamming is shown in Figs. 20-22. In the case of a Rayleigh fading channel (Fig. 20), codes of rate 1/3 perform better than codes of rate 1/2 with any constraint length. For a direct component, Figs. 21-22, codes of rate 1/2 with constraint length $v=7$ perform better than codes of rate 1/3. Hence, over Ricean channels higher rate codes are advantageous.

In Fig. 23 a comparison of the code of rate 1/2 and constraint length of $v=7$ with the uncoded performance for a Rayleigh channel is made. When E_b/N_f is greater than approximately 16 dB, coding improves performance as compared to uncoded performance.

The performance of codes of rate 1/2 and constraint lengths of $v=5, 6$, and 7 are compared with the uncoded performance for a Ricean channel with $a^2/2\sigma^2=5$ in Fig. 24. When E_b/N_f is greater than 15 dB, coded performance is better than the uncoded. In this case the code with constraint length $v=7$ has much better performance than the other two codes examined and is clearly preferable.

Similar results are obtained from the comparison of the performance of codes of rate $1/2$ and constraint lengths of $v=5,6$, and 7 with the uncoded performance for a Ricean channel with $a^2/2\sigma^2=10$, shown in Fig. 25. For E_b/N_I greater than approximately 15 dB, coded performance is better than uncoded. Again in this case, the code with constraint length $v=7$ has much better performance than the other two codes examined and is clearly preferable.

The performance of the system in the presence of partial-band jamming with $\gamma=0.1$ is examined in Figs. 26-28 for three different fading cases. In all cases coded performance is better than uncoded. This especially is true in the case of a Rayleigh fading channel (Fig. 26) where the code with constraint length $v=7$ clearly outperforms the other codes with the same rate of $1/3$ and smaller constraint length. For Ricean fading channels (Figs. 27-28), the code with constraint length $v=7$ is still the optimum compared to other codes with the same rate of $1/2$ and smaller constraint lengths.

C. CONCATENATED CODING

The performance of the system with concatenated codes is now examined. A convolutional code of rate $3/4$ and constraint length of $v=8$ is used as the inner code. Various Reed-Solomon codes are used as outer codes so that the overall code rate is approximately $1/2$. Since the probability of bit error is calculated using union bounds for both the inner and the outer codes, the ratio of bit energy-to-thermal noise E_b/N_0 is taken to be 18 dB to resolve numerical problems in the analysis. The probability of bit error as a function of the bit-to-interference noise energy ratio E_b/N_I is examined for the three different cases of fading channels.

In Figs. 29-30, the performance of the system using Reed-Solomon codes of length 15 and 31 is examined for a Rayleigh fading channel and broadband interference. Concatenated codes with overall rate of approximately 0.55 give the best performance in both cases.

For Ricean fading channels with broadband interference, similar results are obtained (Figs. 31-34). The performance of the system using Reed-Solomon codes of

length 15 and 31 in a Ricean fading channel with $a^2/2\sigma^2=5$ is shown in Figs. 31-32. Using a (15,11) Reed-Solomon code, we obtain a probability of bit error of 10^{-6} with $E_b/N_f=16$ dB (Fig. 31). With the same $E_b/N_f=16$ dB, a probability of bit error of 10^{-7} is obtained using a (31,23) Reed-Solomon code (Fig. 32). As the direct component becomes stronger ($a^2/2\sigma^2=10$), the same probabilities of bit error can be obtained with a slightly less $E_b/N_f=15$ dB and the same outer codes (Fig. 33-34).

A comparison between concatenated codes with the same inner code and different outer codes, but with a similar overall code rate of about 0.55, is shown in Figs. 35-38 for different fading channels and broadband interference. As expected, longer outer codes yield better performance. From this point of view, it is not possible to define an optimum code as performance is dependent on the length of the code. An outer (31,23) Reed-Solomon code gives much better performance than either an outer (15,11) or a (7,5) Reed-Solomon code for a Rayleigh fading channel (Fig. 35). A probability of bit error of 10^{-6} can be obtained with almost 4 dB less in E_b/N_f if an outer (31,23) Reed-Solomon code is used instead of an outer (15,11) Reed-Solomon code.

For Ricean fading channels (Fig. 36-37), the improvement in E_b/N_f is less than 2 dB for the same probability of bit error of 10^{-6} if an outer (31,23) Reed-Solomon code is used instead of an outer (15,11) Reed-Solomon code.

A comparison between the performance of a (31,15) Reed-Solomon code (that is the optimum Reed-Solomon code in this case) and concatenated codes of rate almost 1/2 is made in Fig. 35 for a Rayleigh fading channel and broadband interference. The use of a concatenated code with an outer (31,23) Reed-Solomon code can give a probability of bit error of 10^{-6} with almost 4 dB less E_b/N_f than the (31,15) Reed-Solomon code alone.

In the presence of a direct component (Figs. 36-37), the use of concatenated codes clearly outperforms the (31,17) Reed-Solomon code (that is the optimum Reed-Solomon code in this case) and it is obviously a better choice.

Concatenated codes with outer Reed-Solomon codes of length $n=31$ have been studied in this thesis for theoretical purposes. In practice an outer extended Reed-Solomon

code of length $n=33$ must be used in combination with the rate $3/4$ convolutional inner code in order to resolve synchronization problems.

VII. CONCLUSIONS

An analysis has been presented of the uncoded and coded performance of fast frequency-hopped BFSK receiver with self-normalization combining in a fading channel with partial-band interference. Previously derived expressions [Ref. 9] and [Ref. 2] have been used; and the performance of such a system has been examined for Reed-Solomon codes, convolutional codes, and concatenated codes, all with hard decision decoding, for different channel types and both broadband and partial-band interference.

The application of forward error correction coding improves the performance of such a system and optimum codes have been obtained. The optimum Reed-Solomon codes are consistent with the optimum codes obtained in [Ref. 12], where the coded performance for M-ary FSK modulation in fading channels for a conventional receiver has been examined.

In the analysis performed, the transmitted power and the bit rate are kept fixed and the bit energy is considered to be constant. As a result, an increase in the number of information symbols per code word increases the coded bit energy as well. The increase in coded bit energy allows the use of higher rate codes with better performance in some cases, as it overcomes the advantage of the better error correction that additional redundant bits provide to lower rate codes.

With Reed-Solomon coding, codes of code rates of almost $2/3$ are found to give the best performance in every case examined. Receiver performance is dramatically increased using Reed-Solomon codes of this rate in the presence of partial-band interference.

Convolutional codes of rates $1/2$ and $1/3$ also improve the performance of the receiver compared to the uncoded performance in all cases, but the rates of the codes that can be used and the probabilities of bit error obtained are inferior to those of Reed-Solomon codes.

Concatenated codes with convolutional inner codes, Reed-Solomon outer codes, and overall rate of approximately $1/2$ have also been examined. The performance of the

system using concatenated coding dramatically improves in all cases. Probability of bit error as low as 10^{-6} or 10^{-7} can be obtained. Concatenated codes of relatively small length are found to outperform Reed-Solomon codes in every case.

In conclusion, the application of forward error correction coding in systems with diversity improves the performance of the system and should be used if possible. Concatenated codes give the best performance as compared to Reed-Solomon and convolutional codes of similar code rates, especially for Rayleigh fading channels with broadband interference (the worst case examined). In the presence of partial-band interference, Reed-Solomon codes have good performance and may be applied if the use of concatenated codes is not possible or desired.

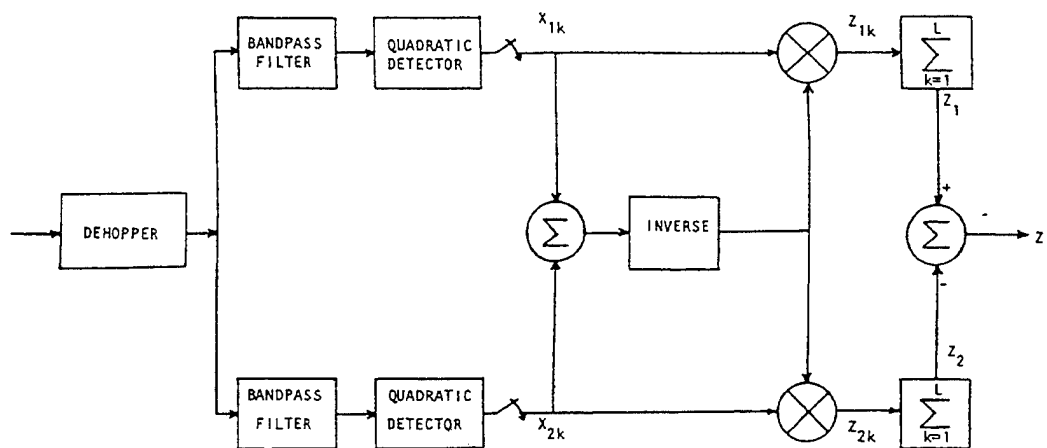


Figure 1. Self-normalization combining FFH/FSK receiver [Ref. 9].

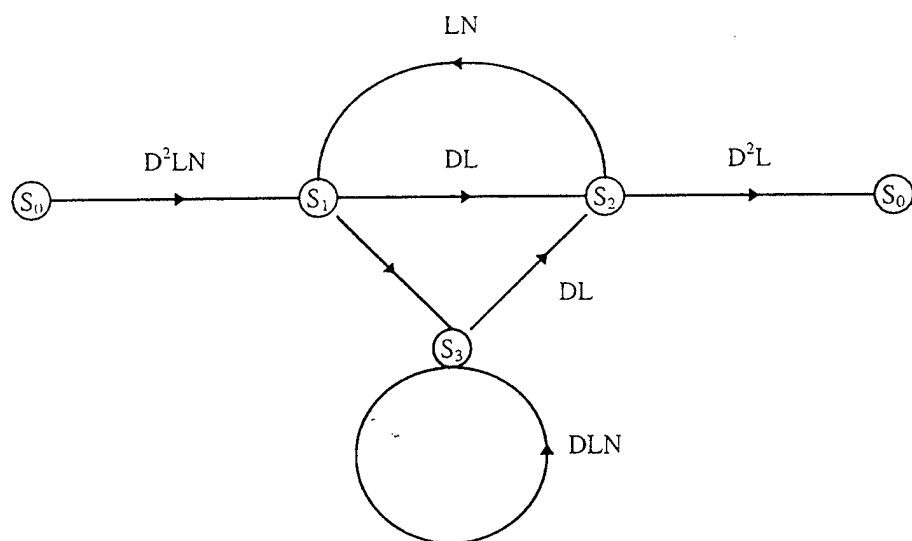


Figure 2. Signal flow diagram for rate 1/2 , constraint length $v=2$ convolutional code [Ref. 6].

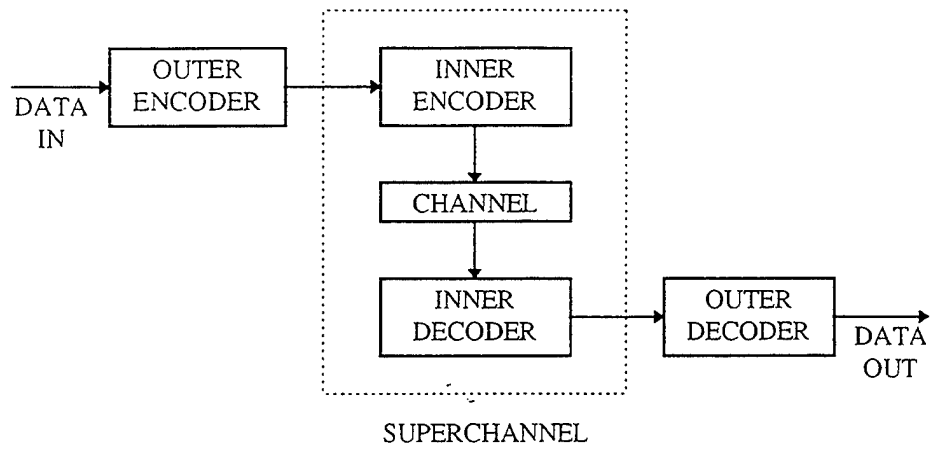


Figure 3. Encoding-decoding approach for concatenated codes [Ref. 6].

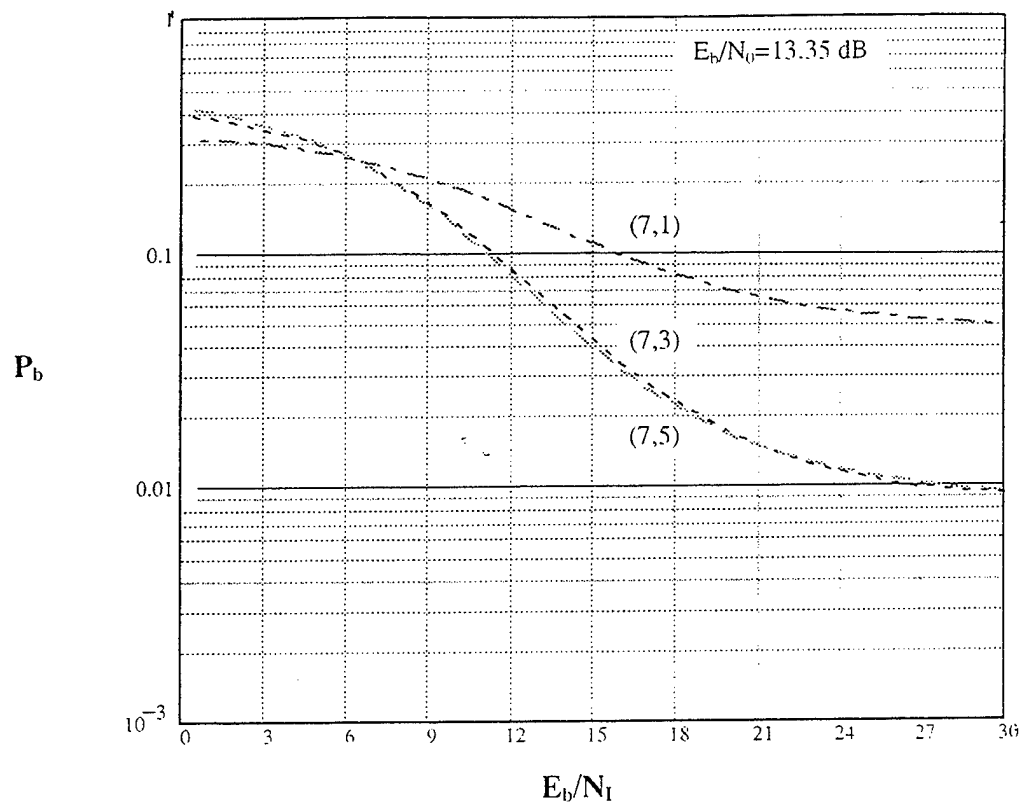


Figure 4. Performance of a fast frequency-hopped BFSK receiver with self-normalization combining in a Rayleigh fading channel ($a^2/2\sigma^2=0$) with Reed-Solomon codes (7,k), diversity $L=4$, and broadband interference.

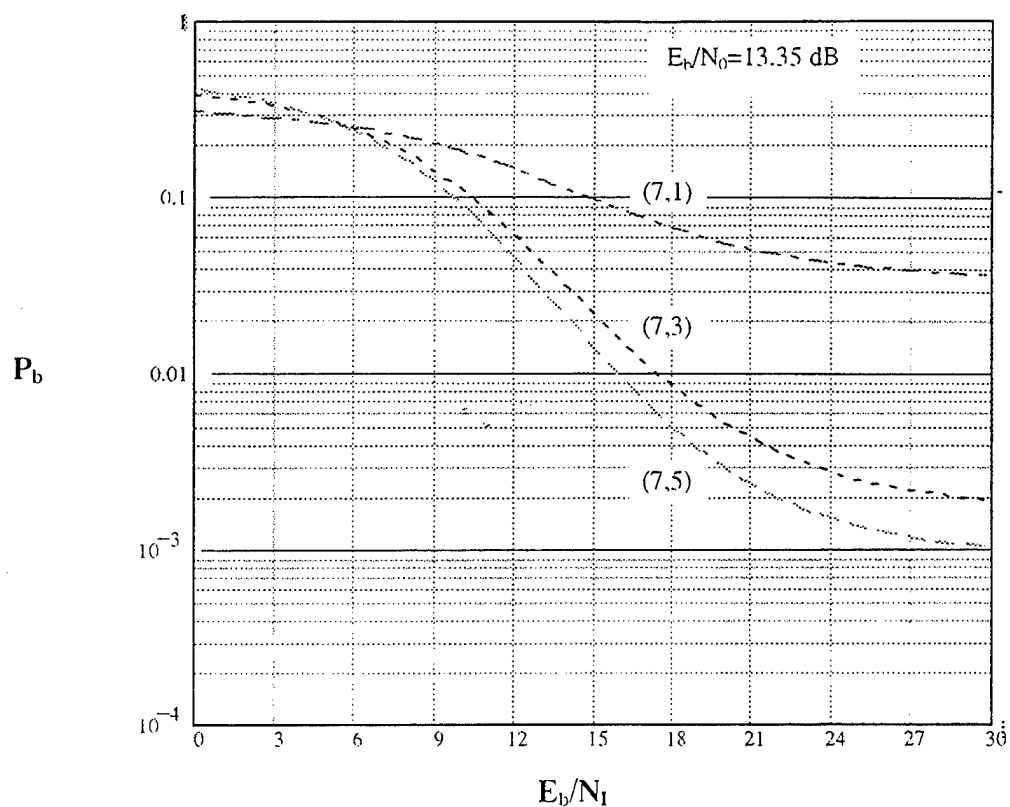


Figure 5. Performance of a fast frequency-hopped BFSK receiver with self-normalization combining in a Ricean fading channel ($a^2/2\sigma^2=5$) with Reed-Solomon codes (7,k), diversity $L=4$, and broadband interference.

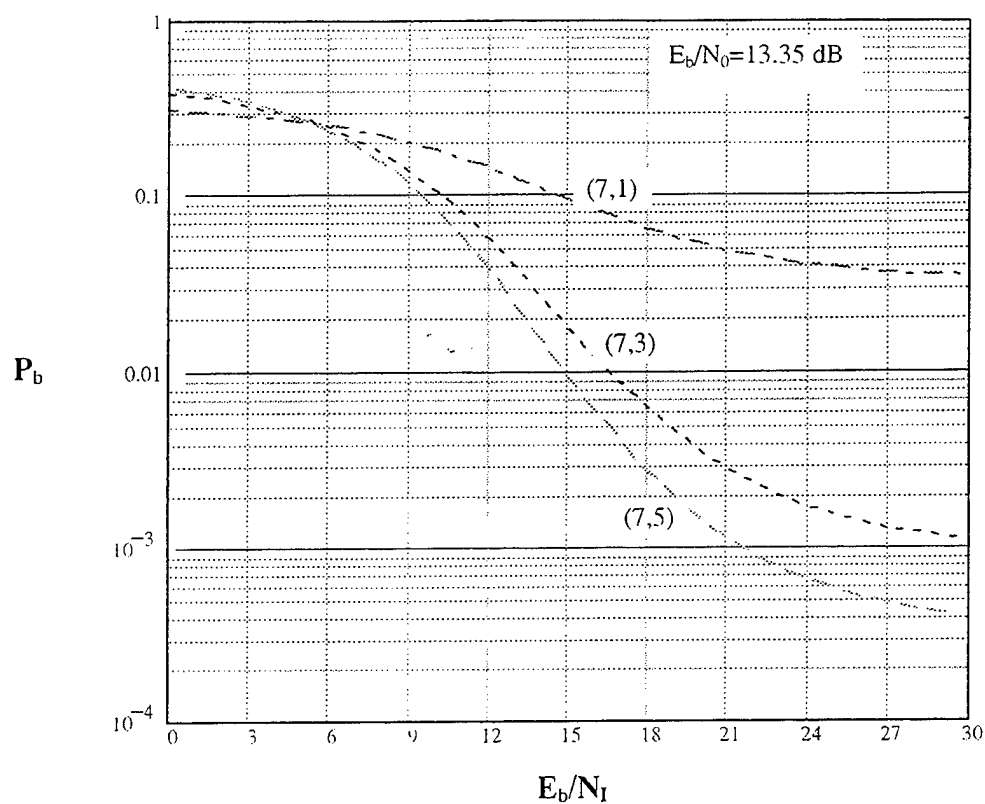


Figure 6. Performance of a fast frequency-hopped BFSK receiver with self-normalization combining in a Ricean fading channel ($a^2/2\sigma^2=10$) with Reed-Solomon codes (7,k), diversity $L=4$, and broadband interference.

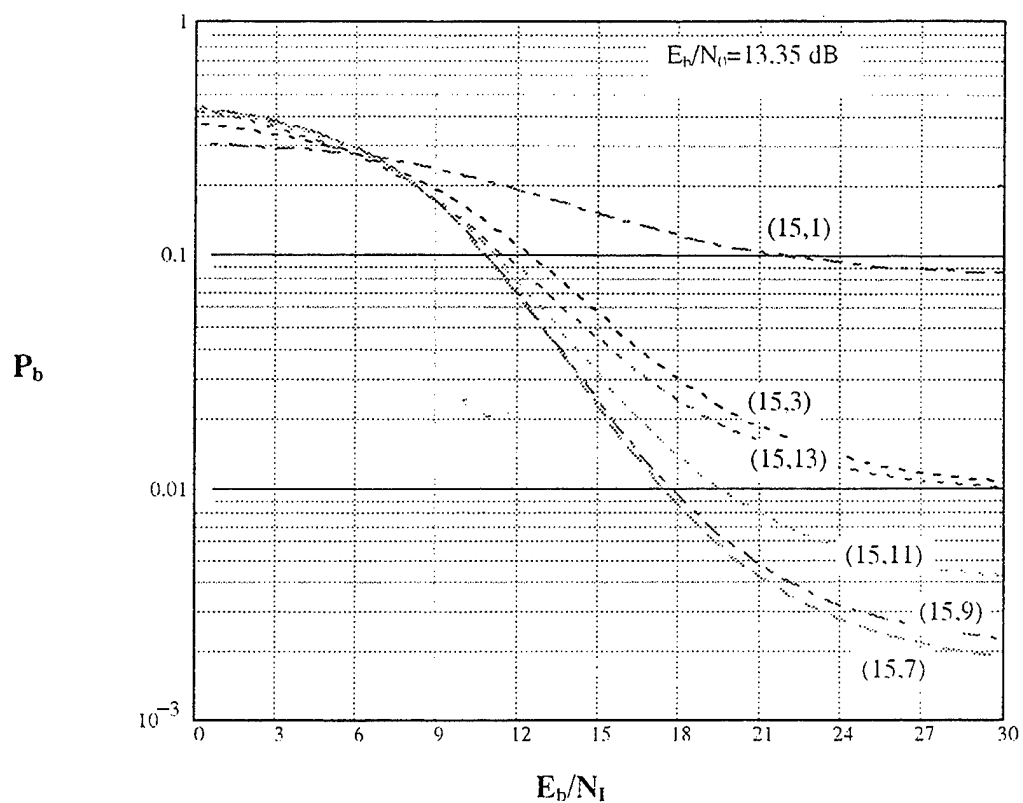


Figure 7. Performance of a fast frequency-hopped BFSK receiver with self-normalization combining in a Rayleigh fading channel ($a^2/2\sigma^2=0$) with Reed-Solomon codes $(15, k)$, diversity $L=4$, and broadband interference.

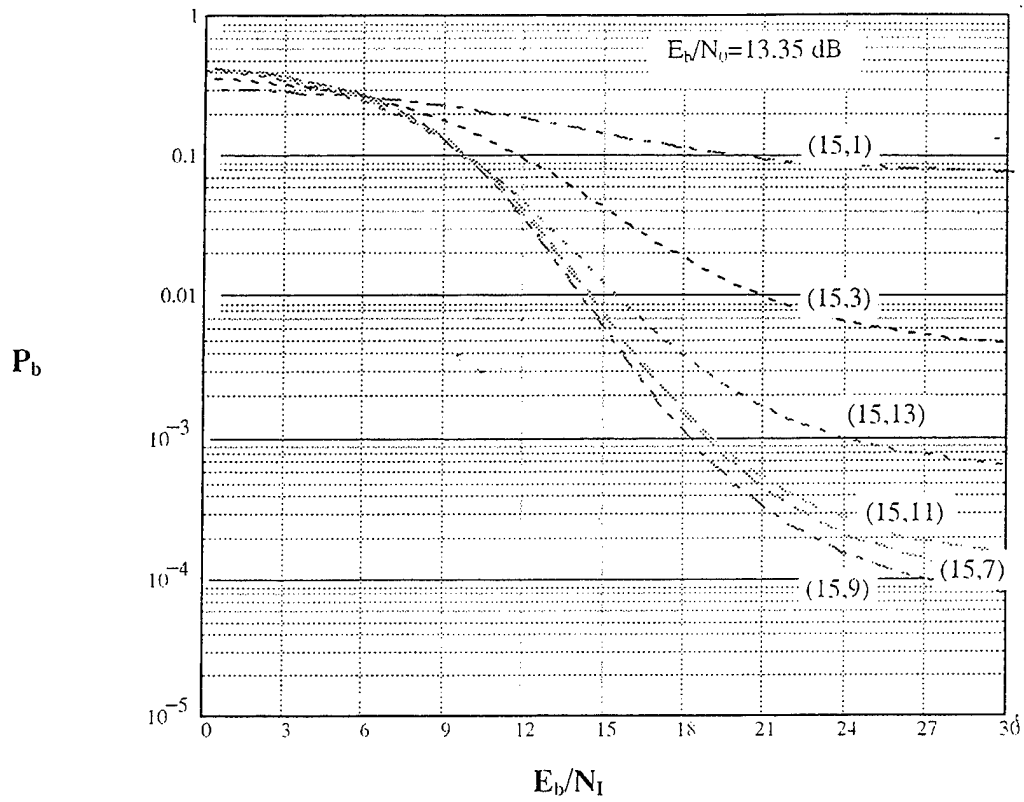


Figure 8. Performance of a fast frequency-hopped BFSK receiver with self-normalization combining in a Ricean fading channel ($a^2/2\sigma^2=5$) with Reed-Solomon codes $(15,k)$, diversity $L=4$, and broadband interference.

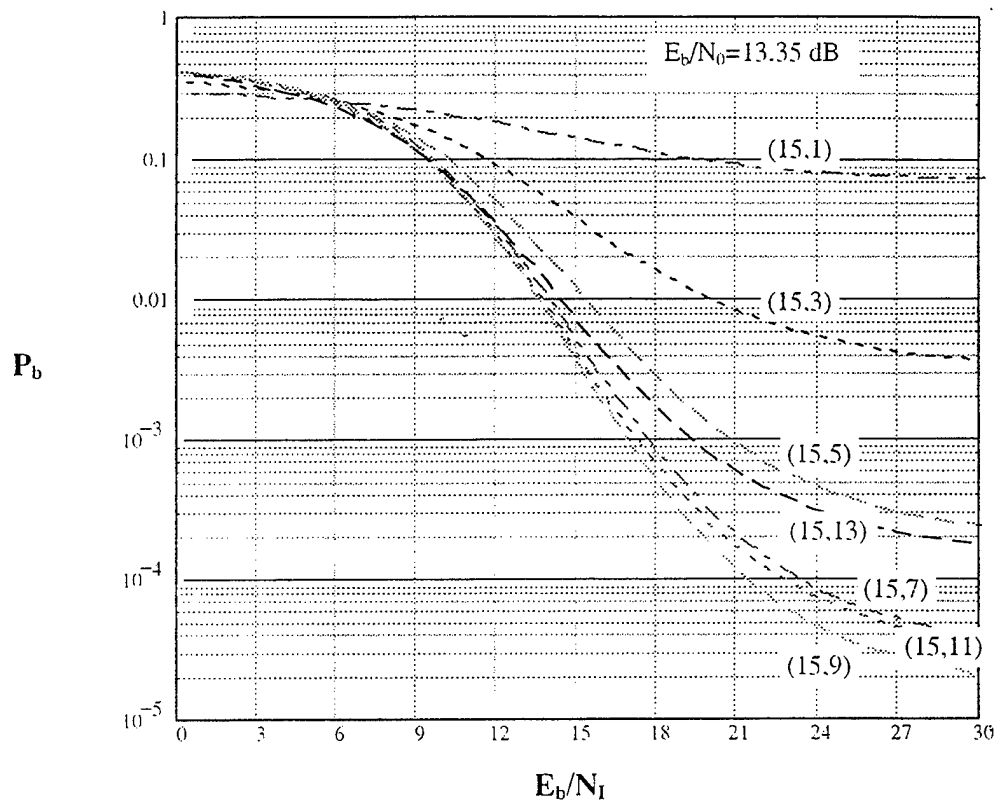


Figure 9. Performance of a fast frequency-hopped BFSK receiver with self-normalization combining in a Ricean fading channel ($a^2/2\sigma^2=10$) with Reed-Solomon codes $(15,k)$, diversity $L=4$, and broadband interference.

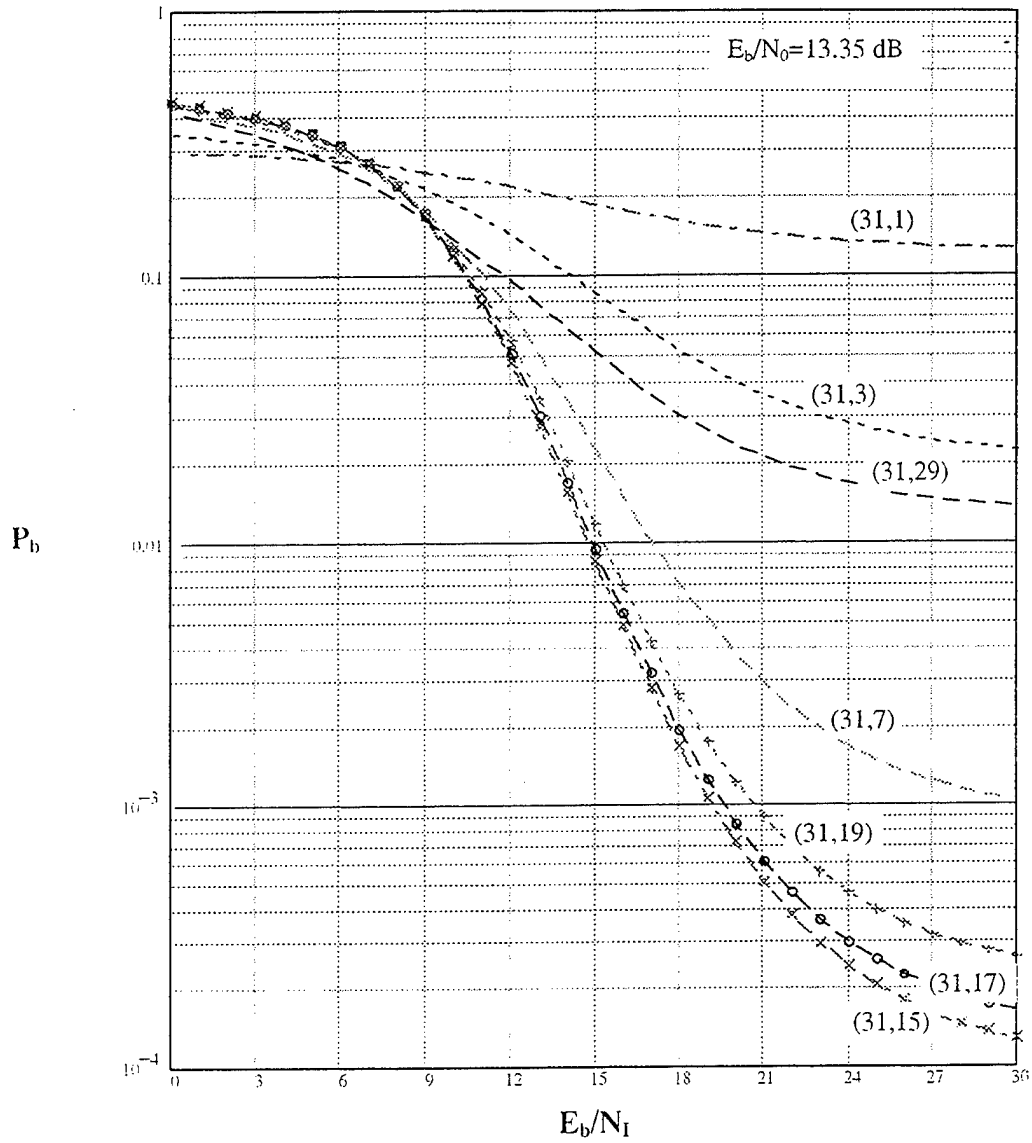


Figure 10. Performance of a fast frequency-hopped BFSK receiver with self-normalization combining in a Rayleigh fading channel ($a^2/2\sigma^2=0$) with Reed-Solomon codes $(31, k)$, diversity $L=4$, and broadband interference.

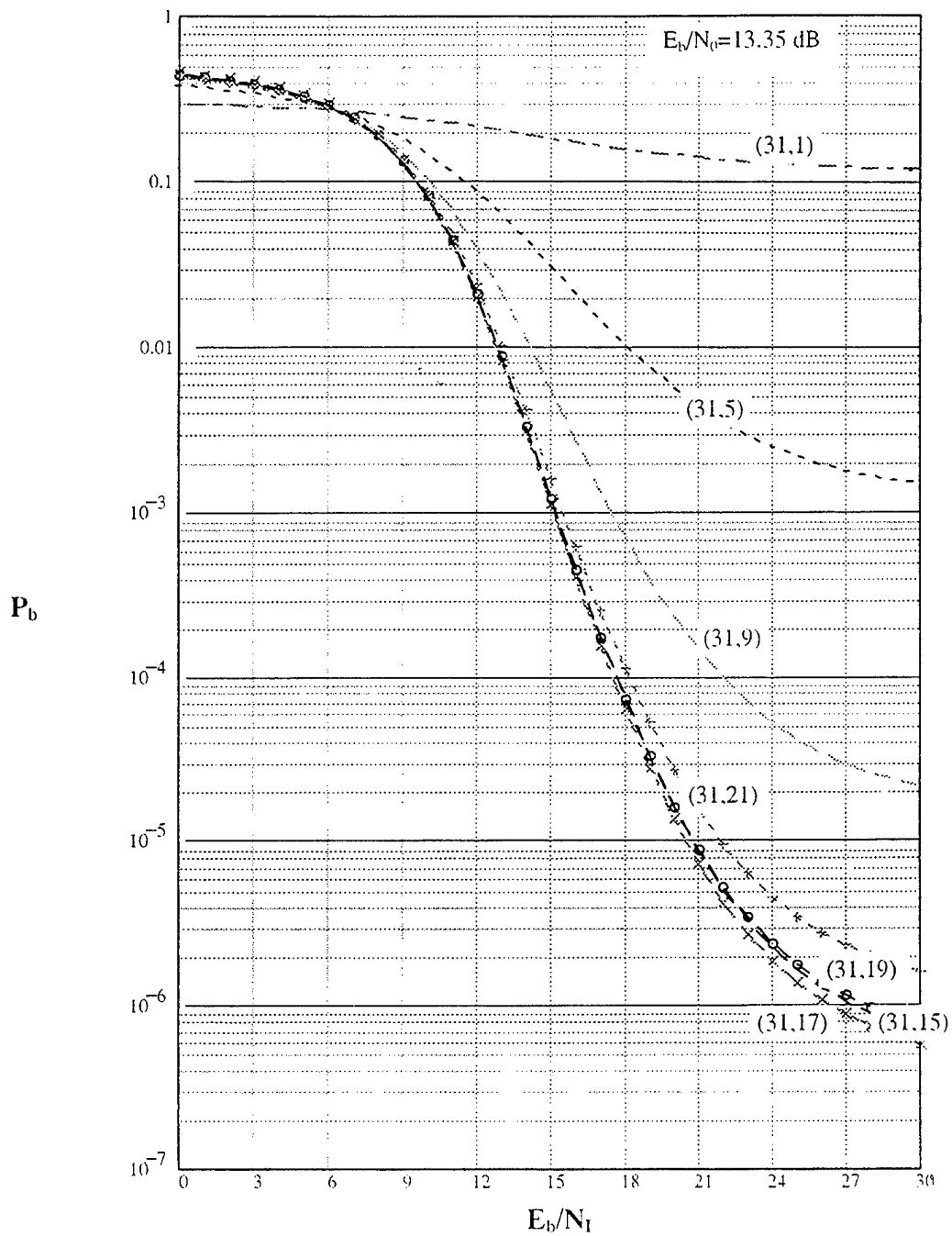


Figure 11. Performance of a fast frequency-hopped BFSK receiver with self-normalization combining in a Ricean fading channel ($a^2/2\sigma^2=5$) with Reed-Solomon codes $(31, k)$, diversity $L=4$, and broadband interference.

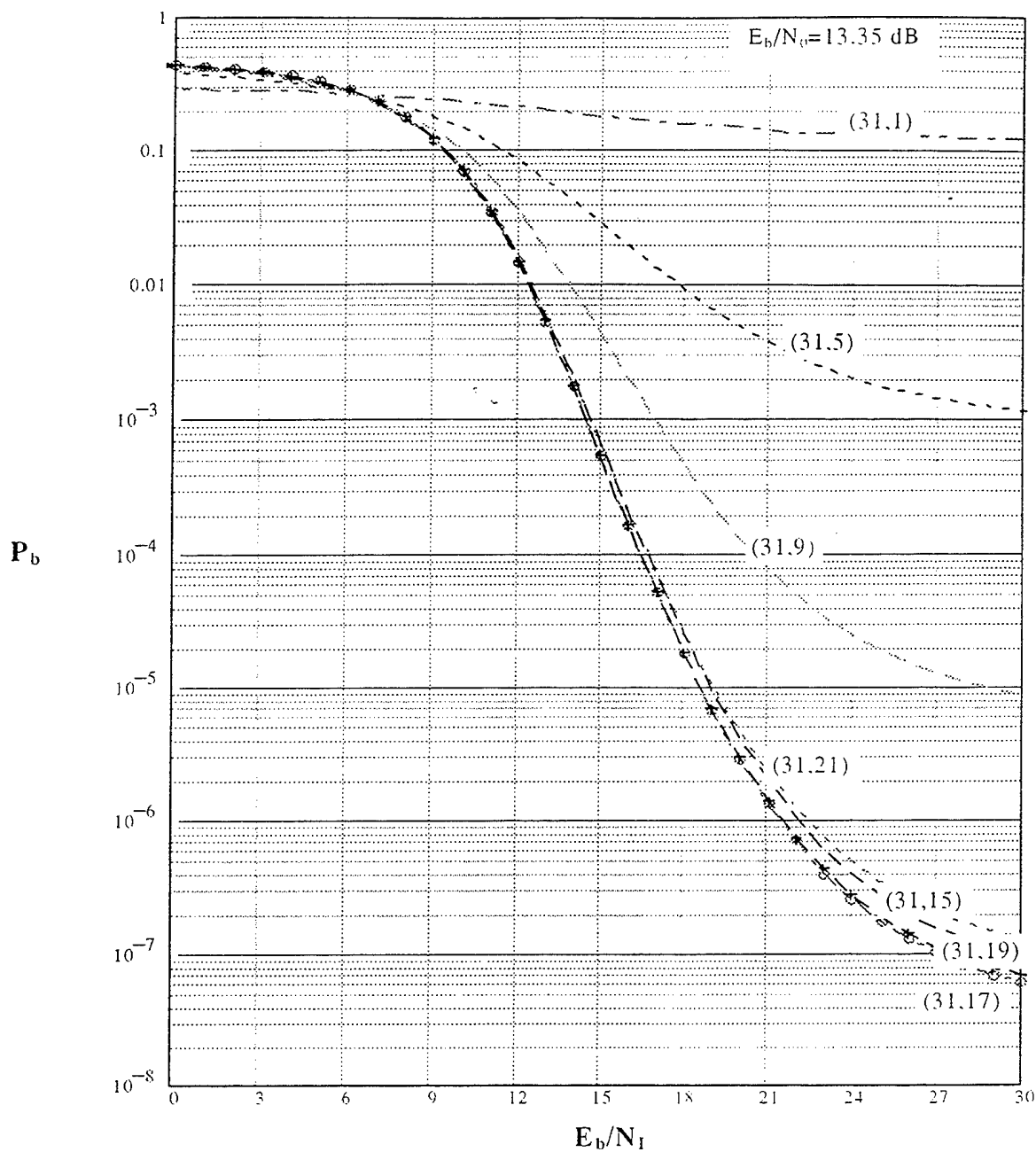


Figure 12. Performance of a fast frequency-hopped BFSK receiver with self-normalization combining in a Rician fading channel ($a^2/2\sigma^2=10$) with Reed-Solomon codes $(31, k)$, diversity $L=4$, and broadband interference.

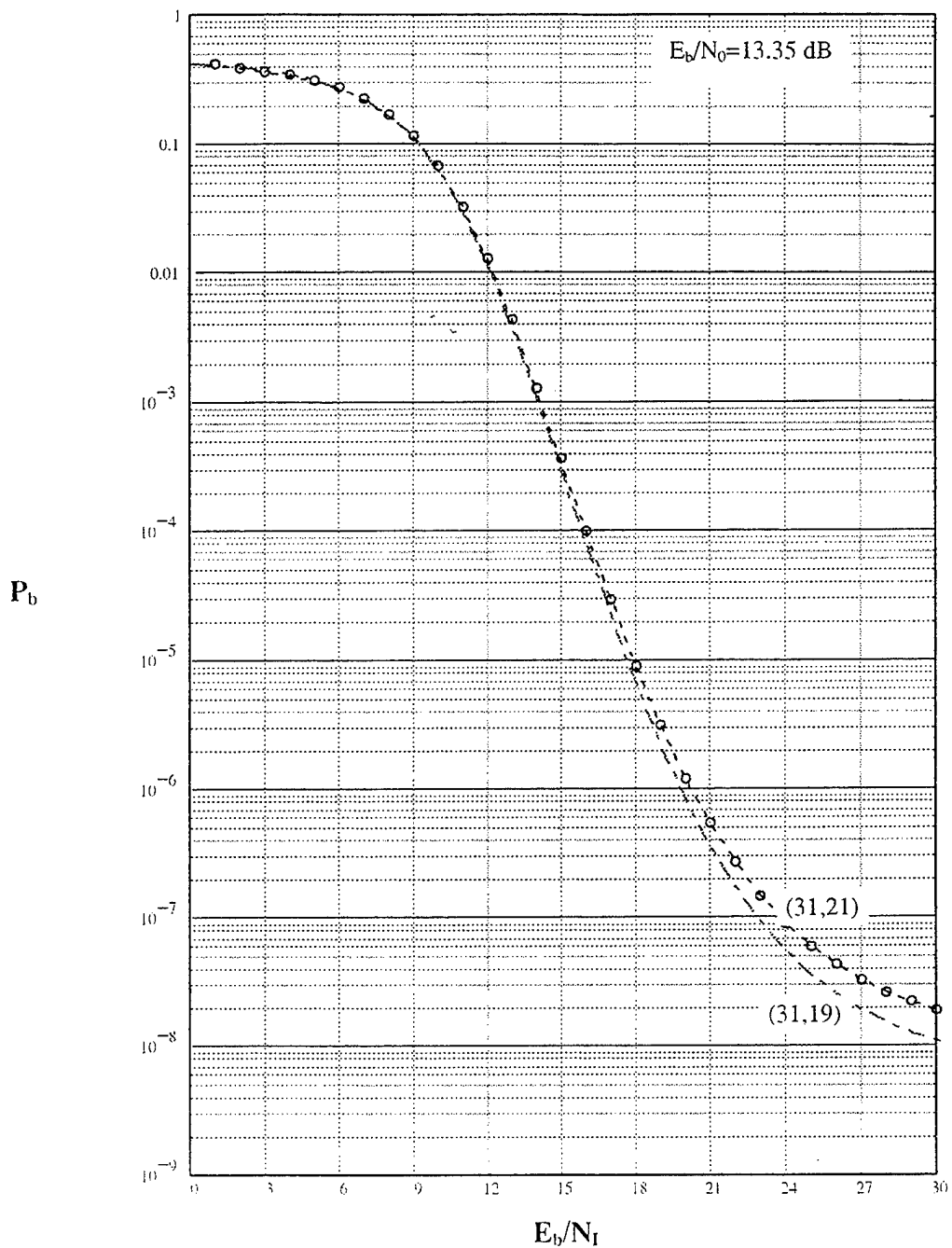


Figure 13. Performance of a fast frequency-hopped BFSK receiver with self-normalization combining in a Ricean fading channel ($a^2/2\sigma^2=20$) with Reed-Solomon codes (31,k), diversity $L=4$, and broadband interference.

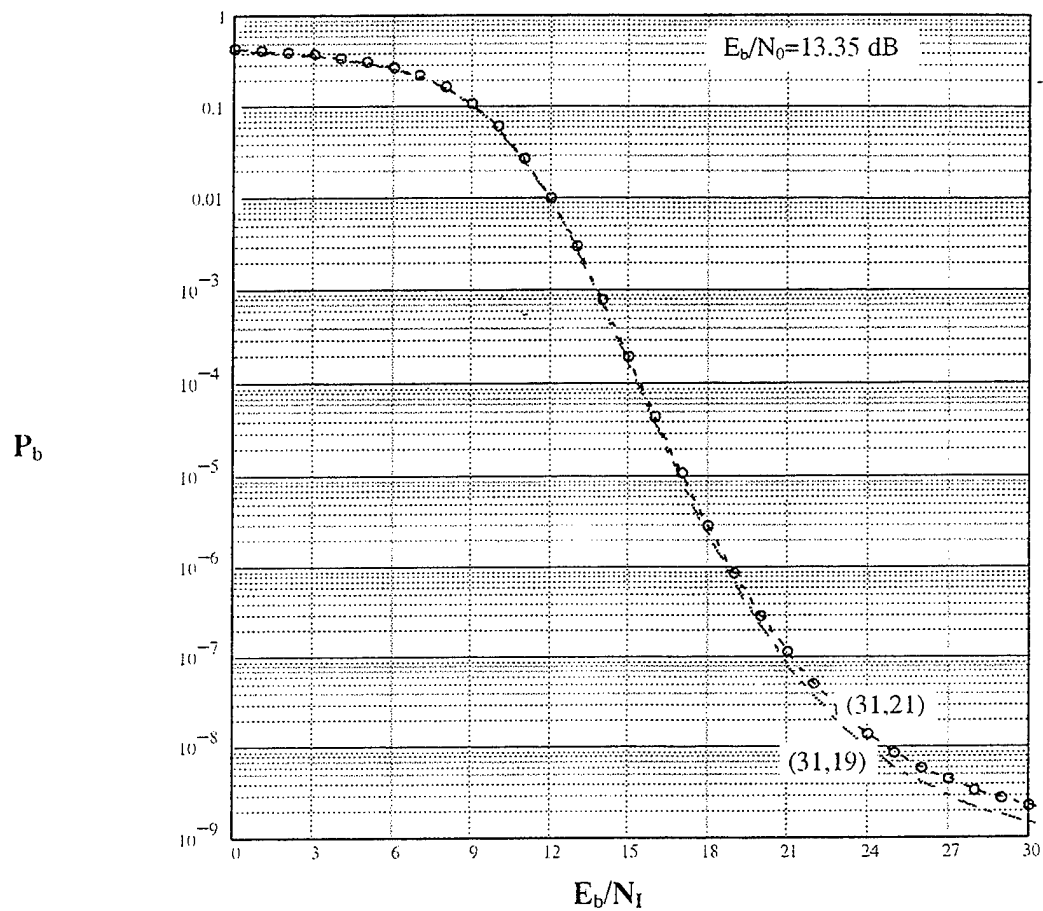


Figure 14. Performance of a fast frequency-hopped BFSK receiver with self-normalization combining in a Ricean fading channel ($a^2/2\sigma^2=100$) with Reed-Solomon codes (31,k), diversity $L=4$, and broadband interference.

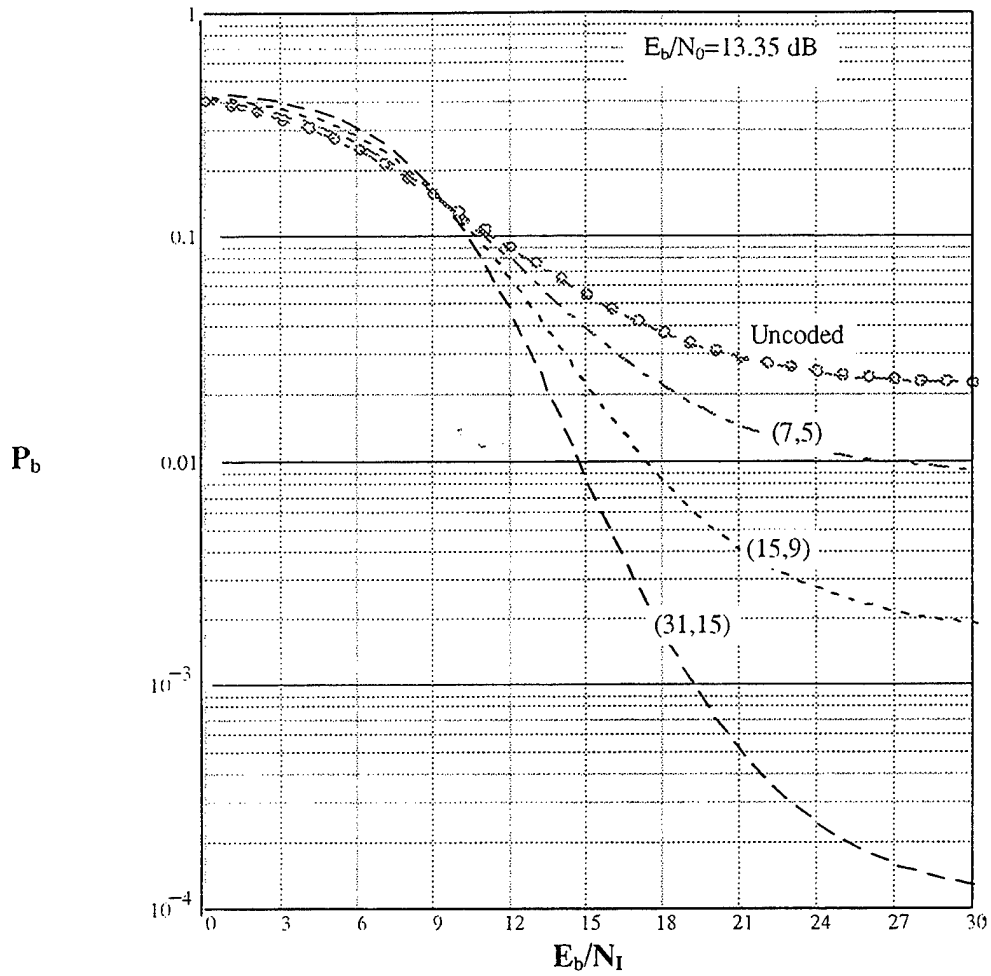


Figure 15. Optimum Reed-Solomon codes of length $n=7,15,31$ and uncoded performance comparison for a Rayleigh fading channel ($a^2/2\sigma^2=0$) with diversity $L=4$, and broadband interference.

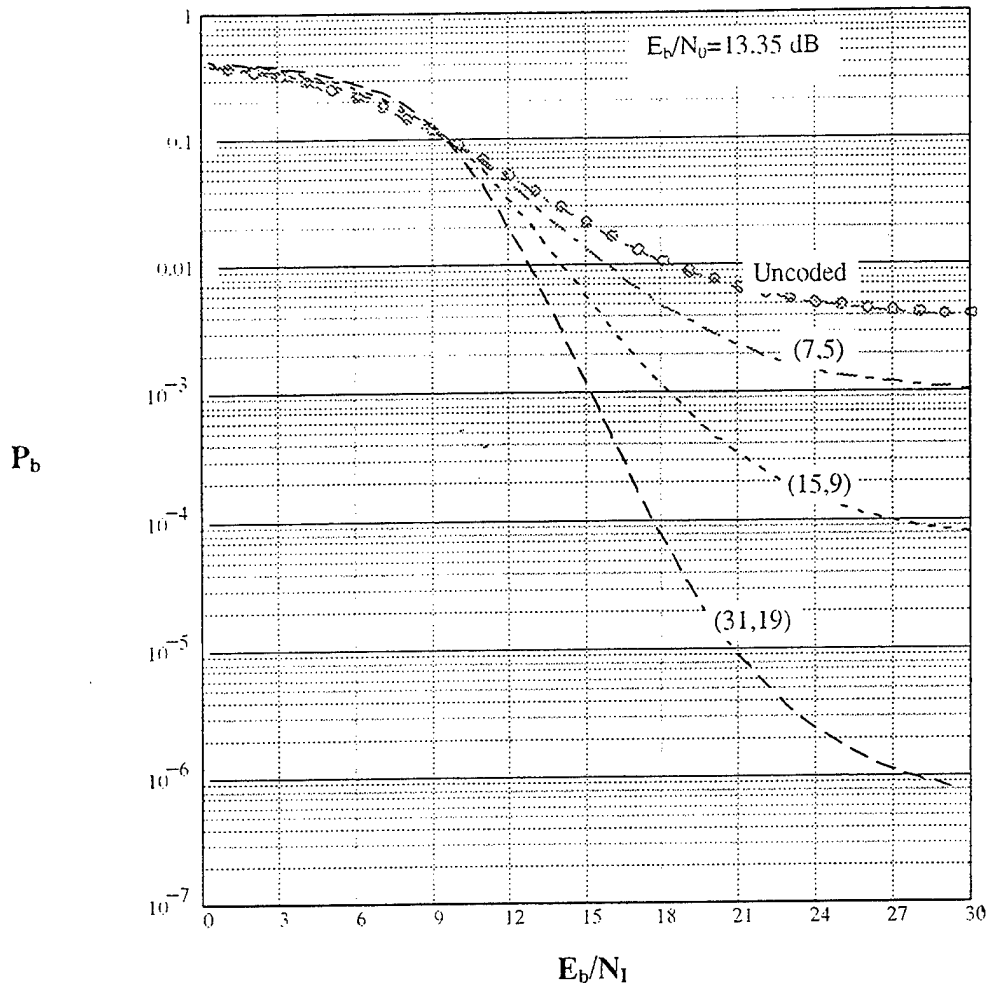


Figure 16. Optimum Reed-Solomon codes of length $n=7, 15, 31$ and uncoded performance comparison for a Ricean fading channel ($a^2/2\sigma^2=5$) with diversity $L=4$, and broadband interference.

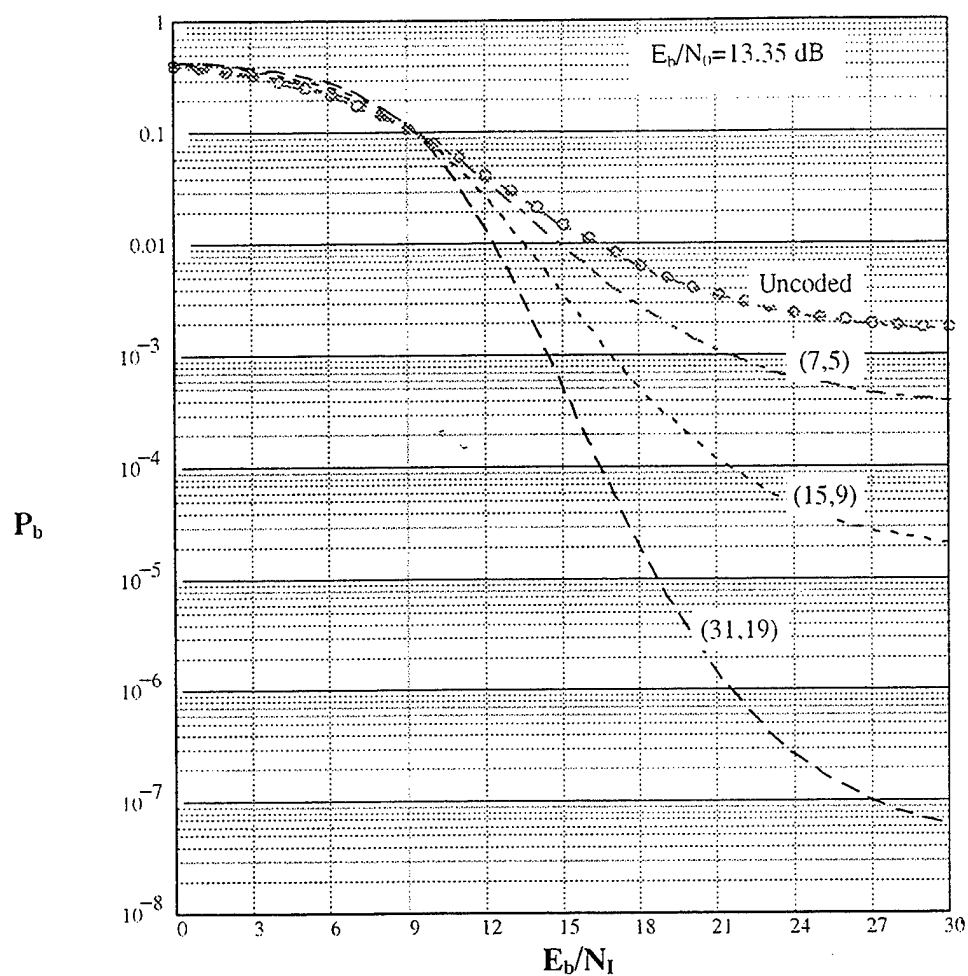


Figure 17. Optimum Reed-Solomon codes of length $n=7,15,31$ and uncoded performance comparison for a Ricean fading channel ($a^2/2\sigma^2=10$) with diversity $L=4$, and broadband interference.

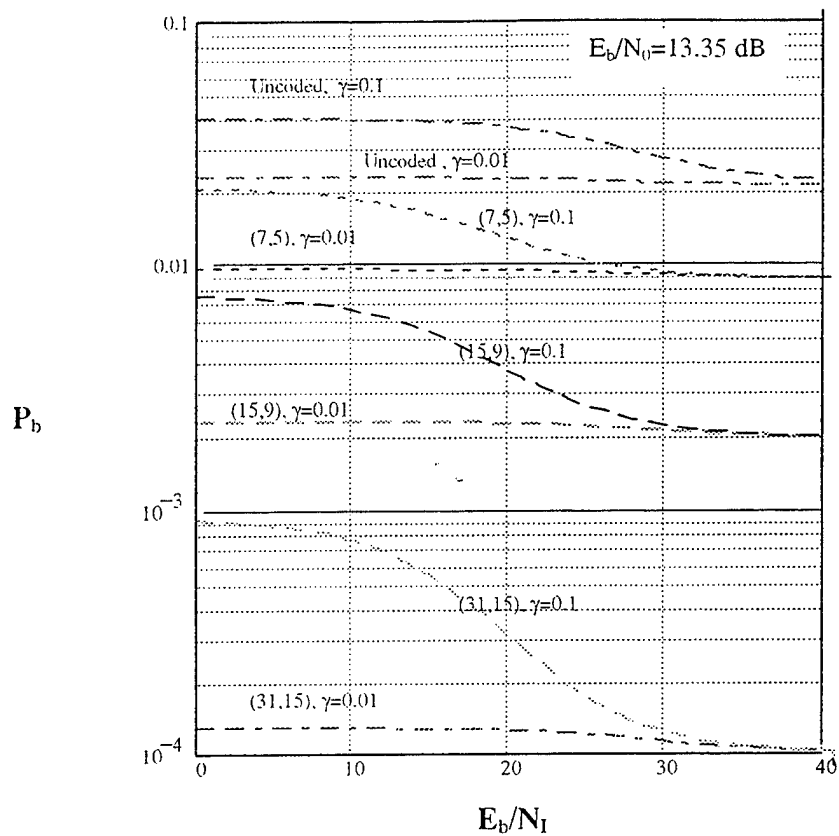


Figure 18. Optimum Reed-Solomon codes of length $n=7,15,31$ and uncoded performance comparison for a Rayleigh fading channel ($a^2/2\sigma^2=0$) with diversity $L=4$, and partial-band interference.

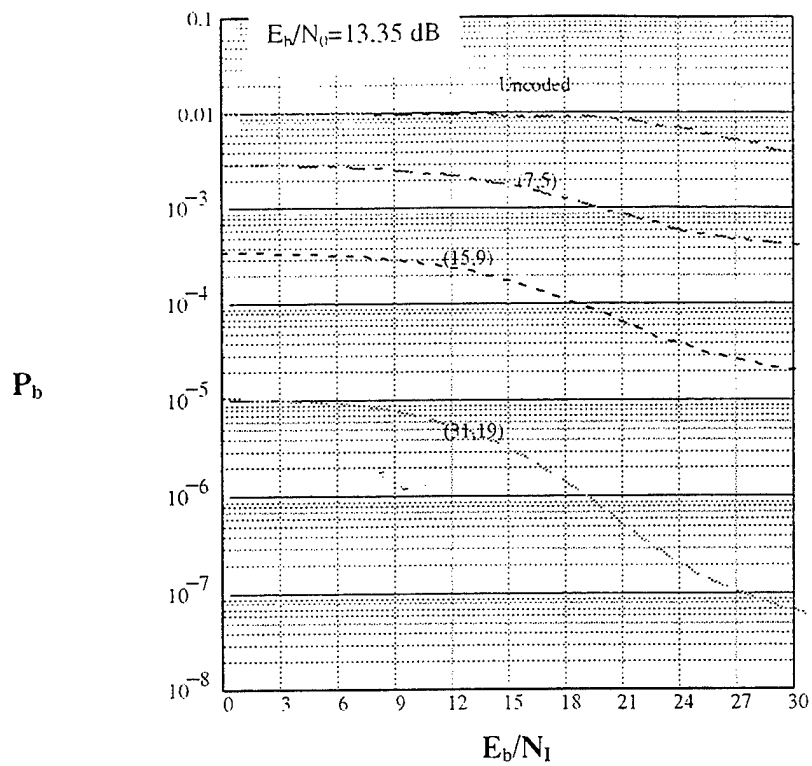


Figure 19. Optimum Reed-Solomon codes of length $n=7, 15, 31$ and uncoded performance comparison for a Ricean fading channel ($a^2/2\sigma^2=10$) with diversity $L=4$, and partial-band interference ($\gamma=0.1$).

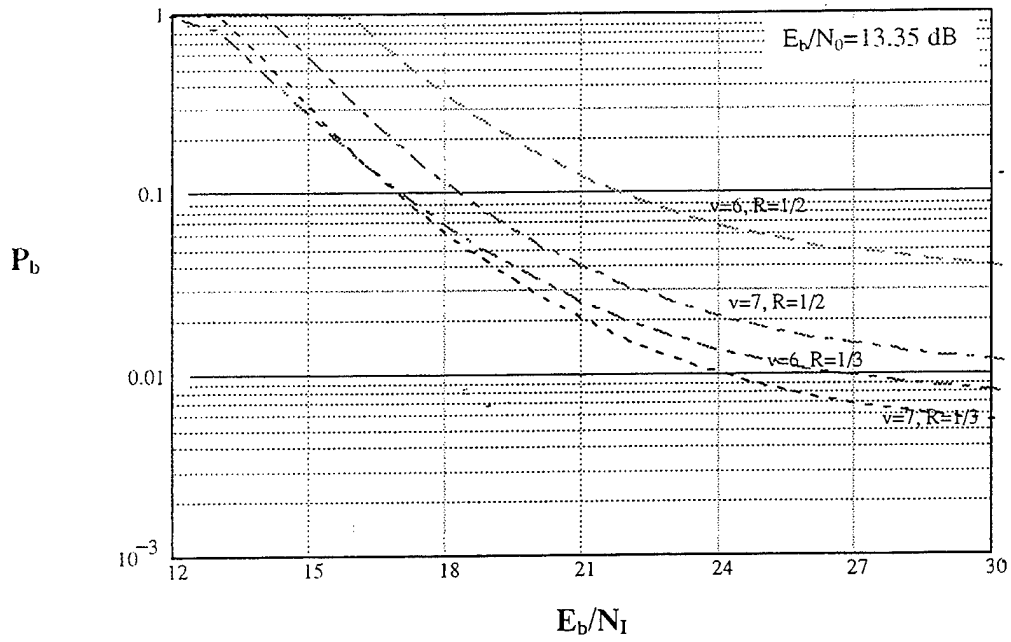


Figure 20. Performance of a fast frequency-hopped BFSK receiver with self-normalization combining in a Rayleigh fading channel ($a^2/2\sigma^2=0$) with convolutional coding, diversity $L=4$, and broadband interference.

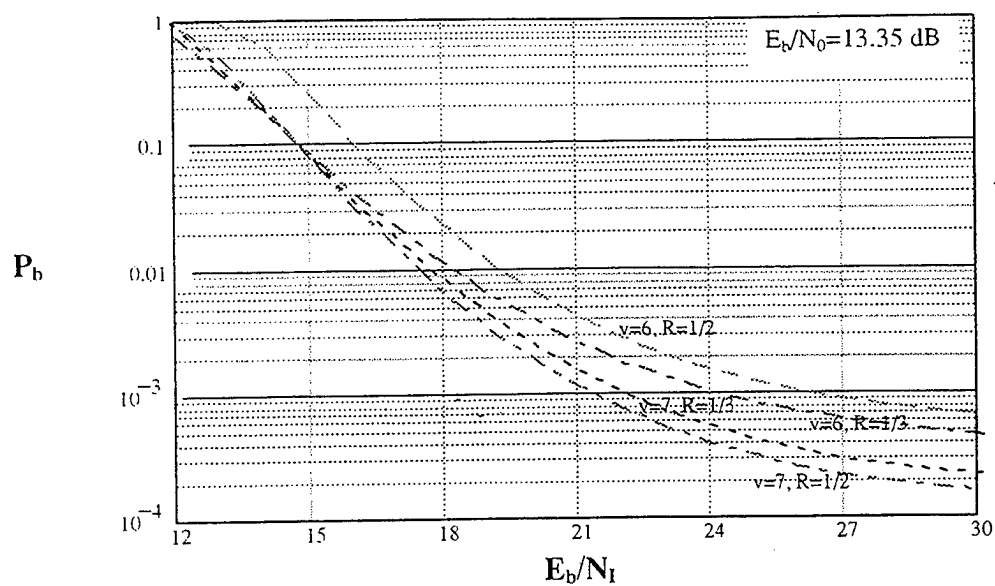


Figure 21. Performance of a fast frequency-hopped BFSK receiver with self-normalization combining in a Ricean fading channel ($a^2/2\sigma^2=5$) with convolutional coding, diversity $L=4$, and broadband interference.

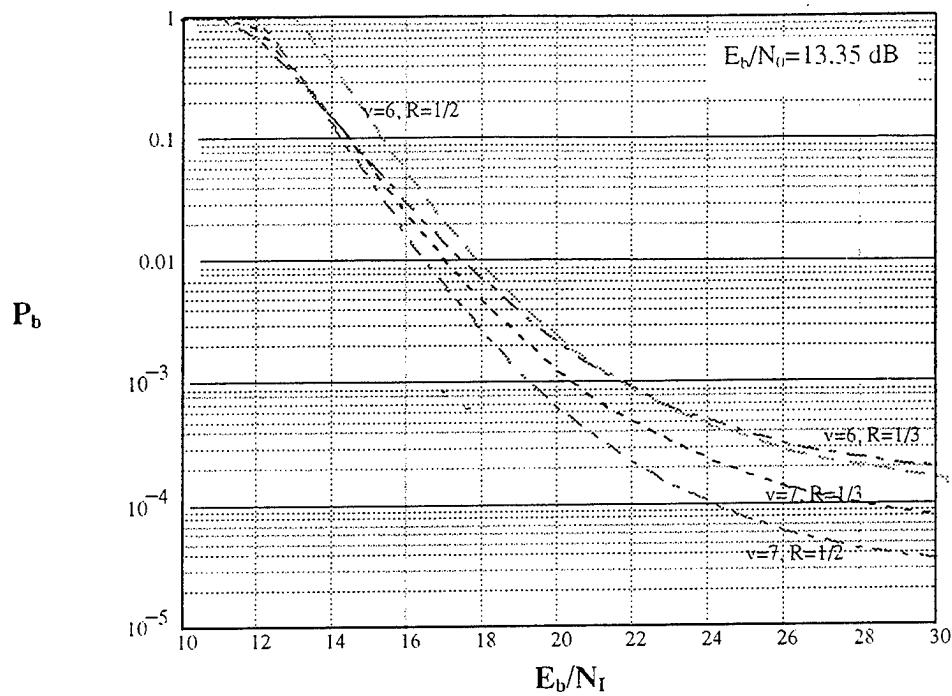


Figure 22. Performance of a fast frequency-hopped BFSK receiver with self-normalization combining in a Ricean fading channel ($a^2/2\sigma^2=10$) with convolutional coding, diversity $L=4$, and broadband interference.

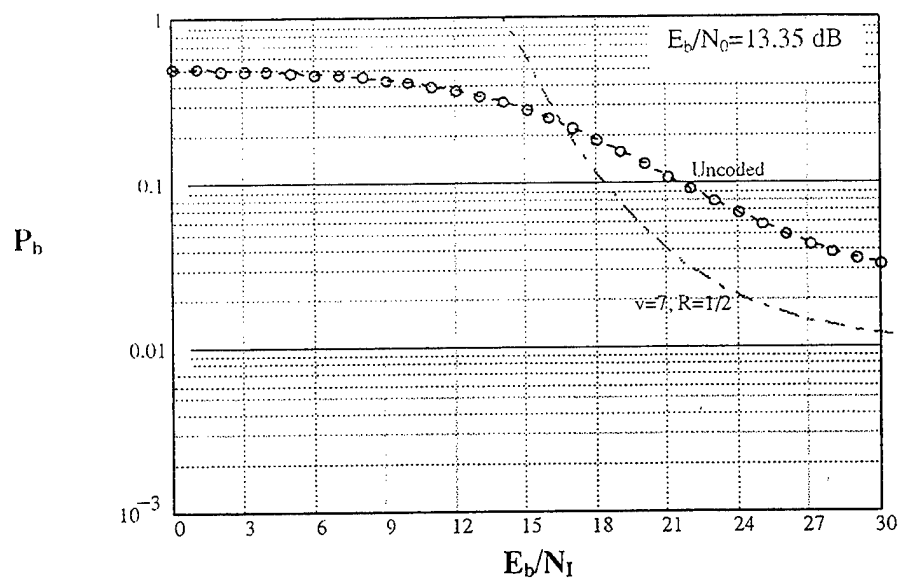


Figure 23. Optimum convolutional code of rate 1/2 and uncoded performance comparison for a Rayleigh fading channel ($a^2/2\sigma^2=0$) with diversity $L=4$, and broadband interference.

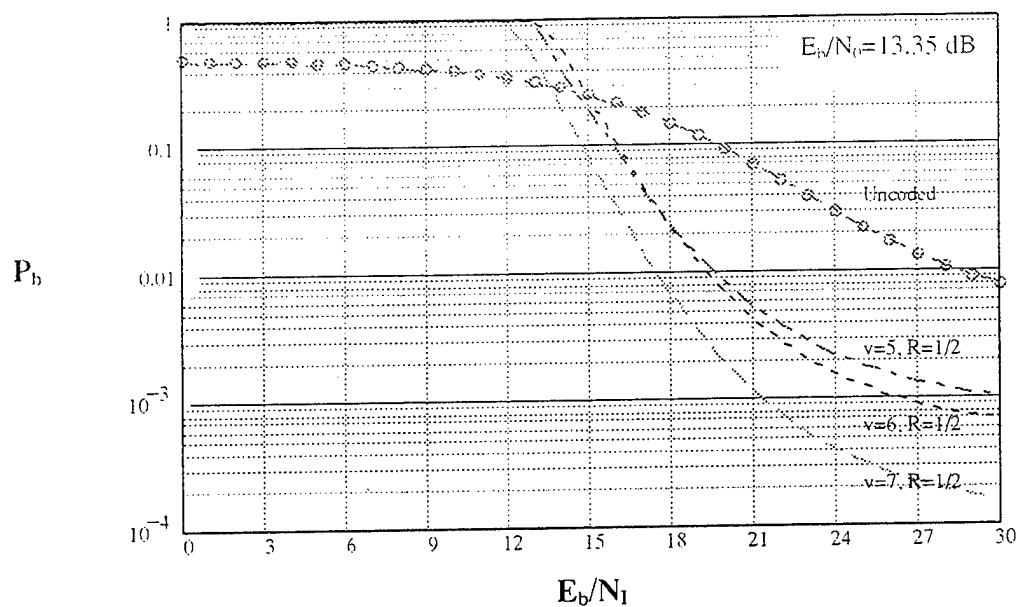


Figure 24. Optimum convolutional codes of rate 1/2 and uncoded performance comparison for a Ricean fading channel ($a^2/2\sigma^2=5$) with diversity $L=4$, and broadband interference.

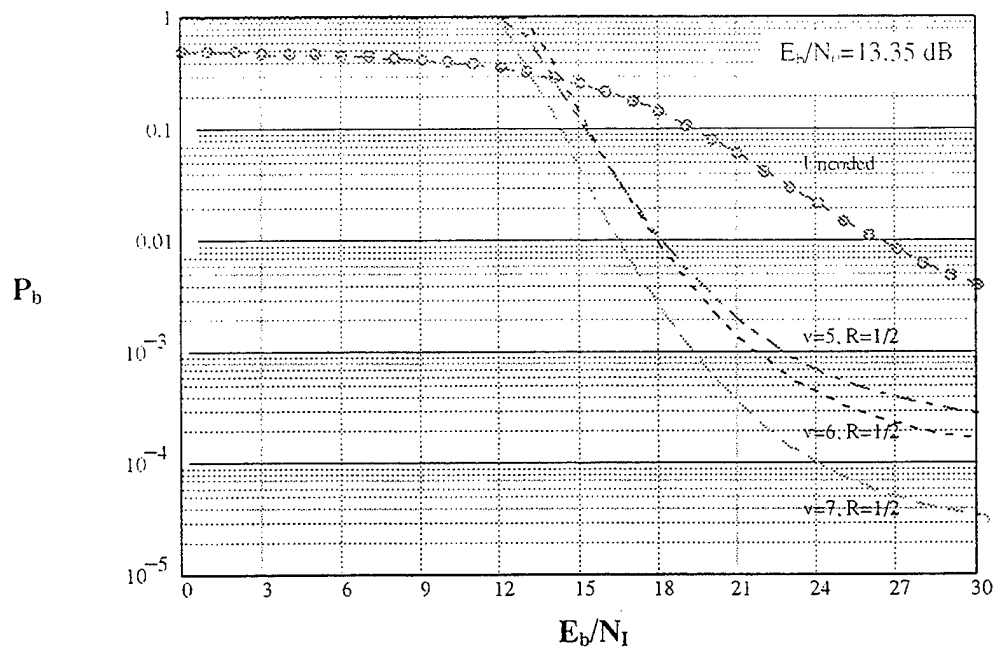


Figure 25. Optimum convolutional codes of rate 1/2 and uncoded performance comparison for a Ricean fading channel ($a^2/2\sigma^2=10$) with diversity $L=4$, and broadband interference.

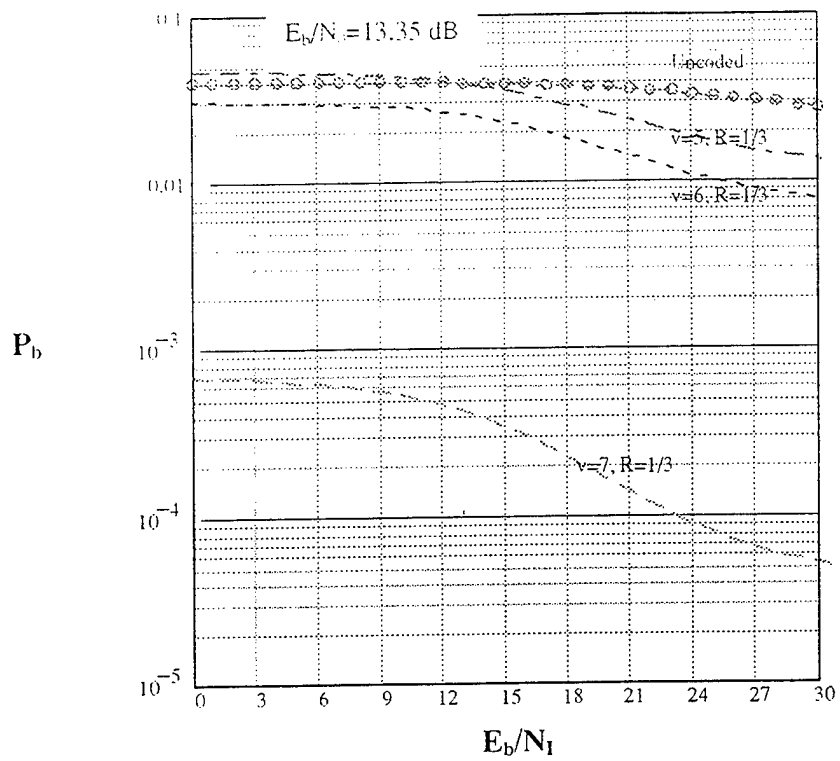


Figure 26. Optimum convolutional codes of rate 1/3 and uncoded performance comparison for a Rayleigh fading channel ($\alpha^2/2\sigma^2=0$) with diversity $L=4$, and partial-band interference.

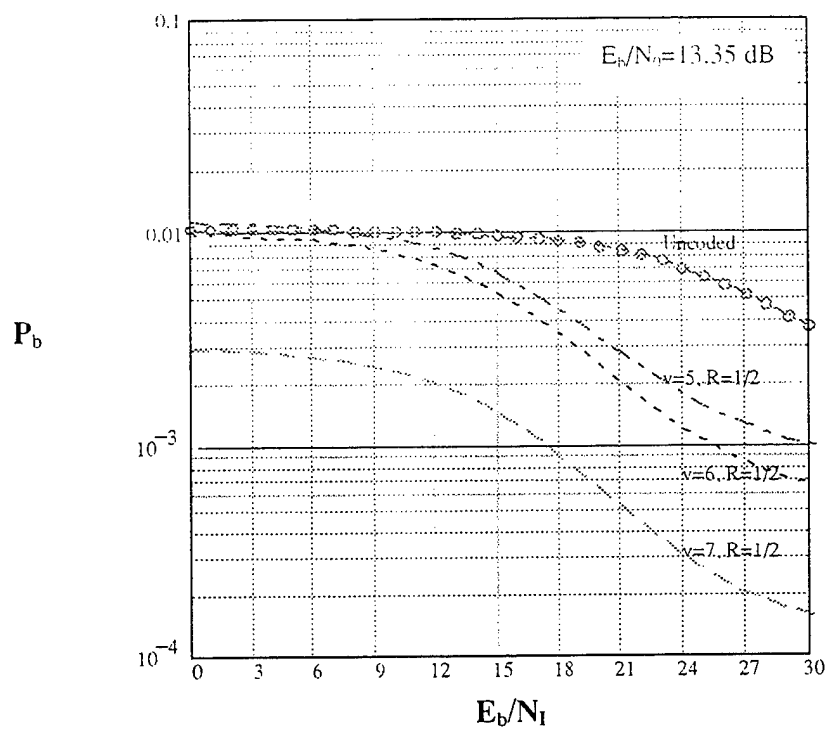


Figure 27. Optimum convolutional codes of rate 1/2 and uncoded performance comparison for a Ricean fading channel ($a^2/2\sigma^2=5$) with diversity $L=4$, and partial-band interference ($\gamma=0.1$).

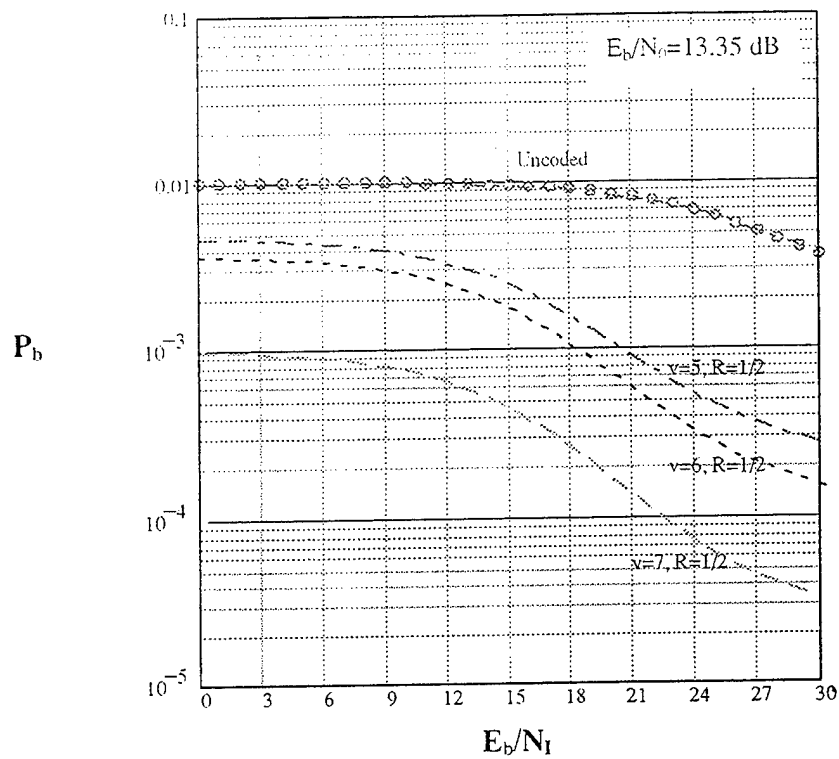


Figure 28. Optimum convolutional codes of rate 1/2 and uncoded performance comparison for a Ricean fading channel ($a^2/2\sigma^2=10$) with diversity $L=4$, and partial-band interference ($\gamma=0.1$).

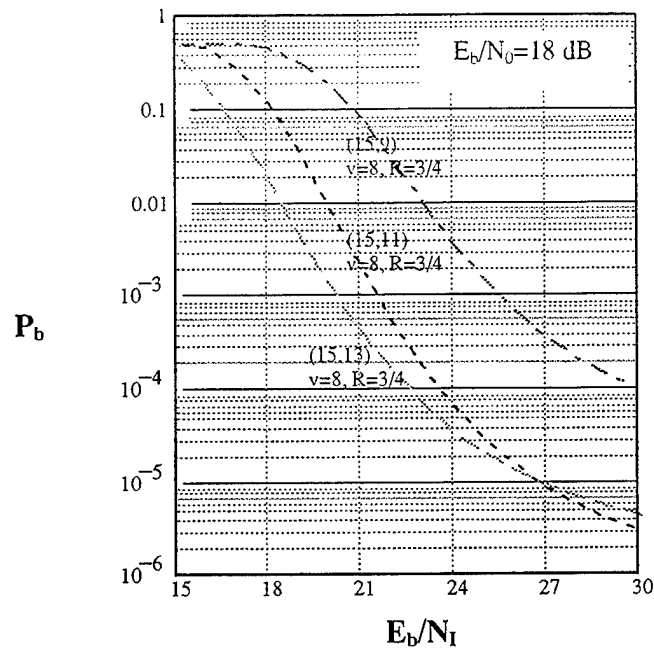


Figure 29. Performance of a fast frequency-hopped BFSK receiver with self-normalization combining in a Rayleigh fading channel ($a^2/2\sigma^2=0$) with concatenated coding, diversity $L=4$, and broadband interference.

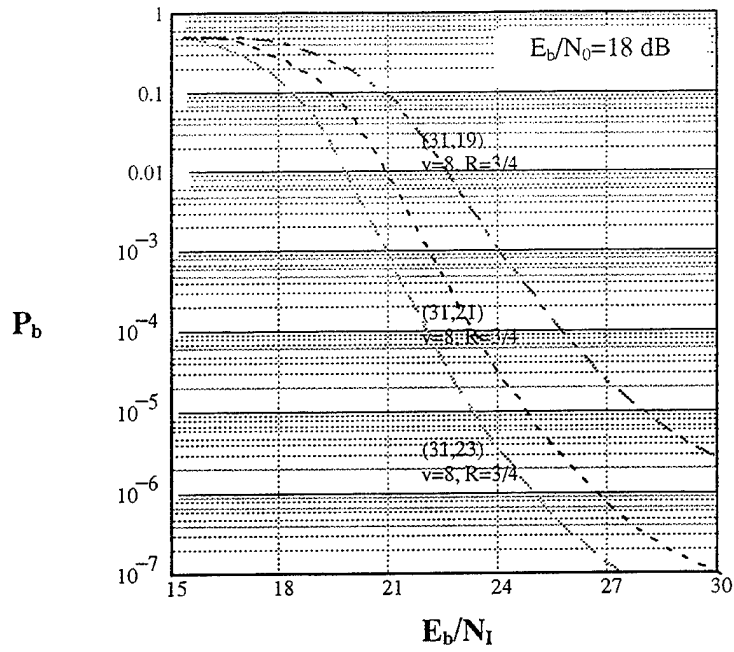


Figure 30. Performance of a fast frequency-hopped BFSK receiver with self-normalization combining in a Rayleigh fading channel ($\alpha^2/2\sigma^2=0$) with concatenated coding, diversity $L=4$, and broadband interference.

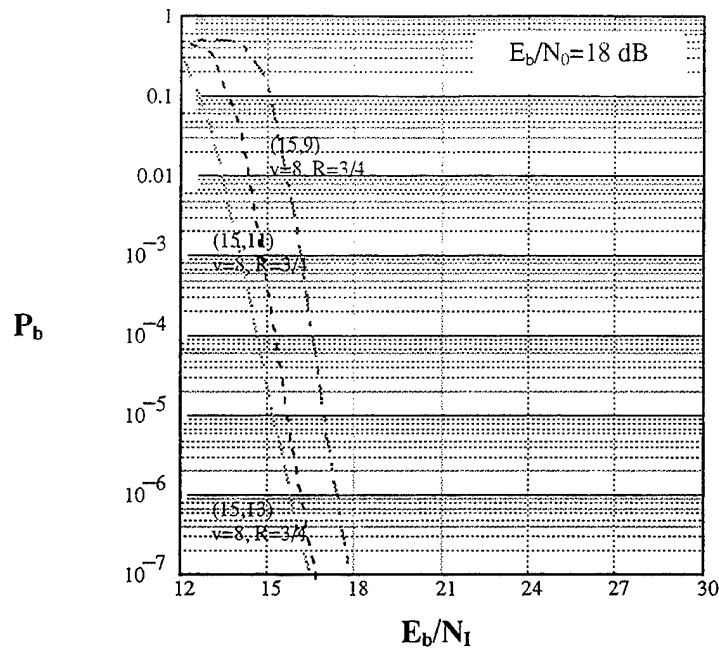


Figure 31. Performance of a fast frequency-hopped BFSK receiver with self-normalization combining in a Ricean fading channel ($a^2/2\sigma^2=5$) with concatenated coding, diversity $L=4$, and broadband interference.

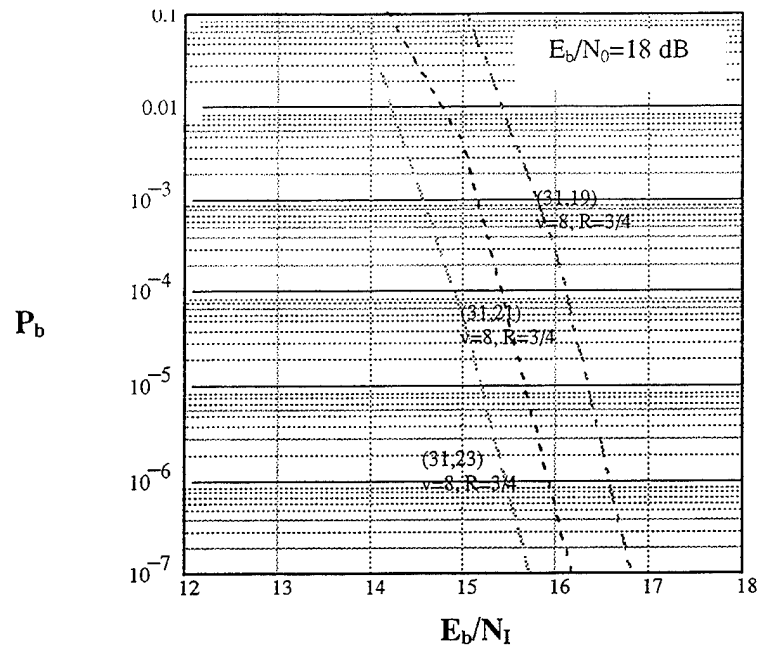


Figure 32. Performance of a fast frequency-hopped BFSK receiver with self-normalization combining in a Ricean fading channel ($a^2/2\sigma^2=5$) with concatenated coding, diversity $L=4$, and broadband interference.

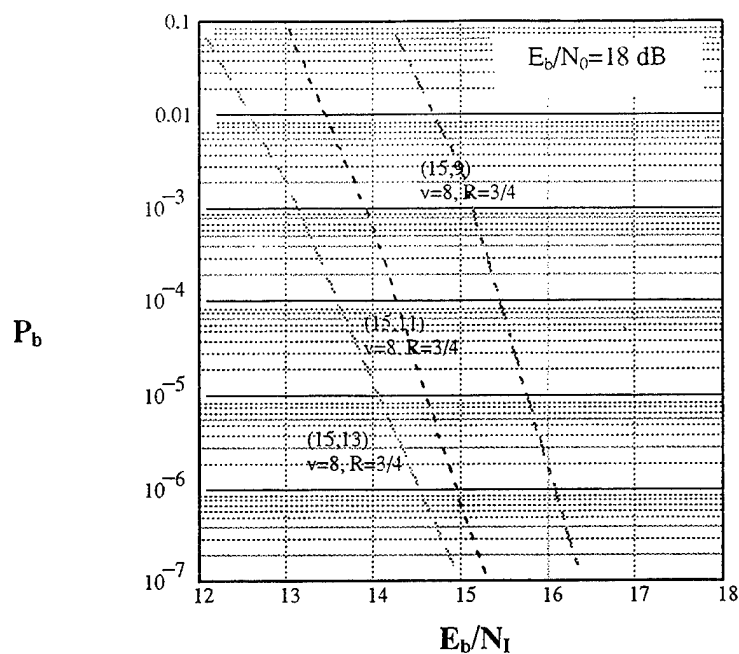


Figure 33. Performance of a fast frequency-hopped BFSK receiver with self-normalization combining in a Ricean fading channel ($a^2/2\sigma^2=10$) with concatenated coding, diversity $L=4$, and broadband interference.

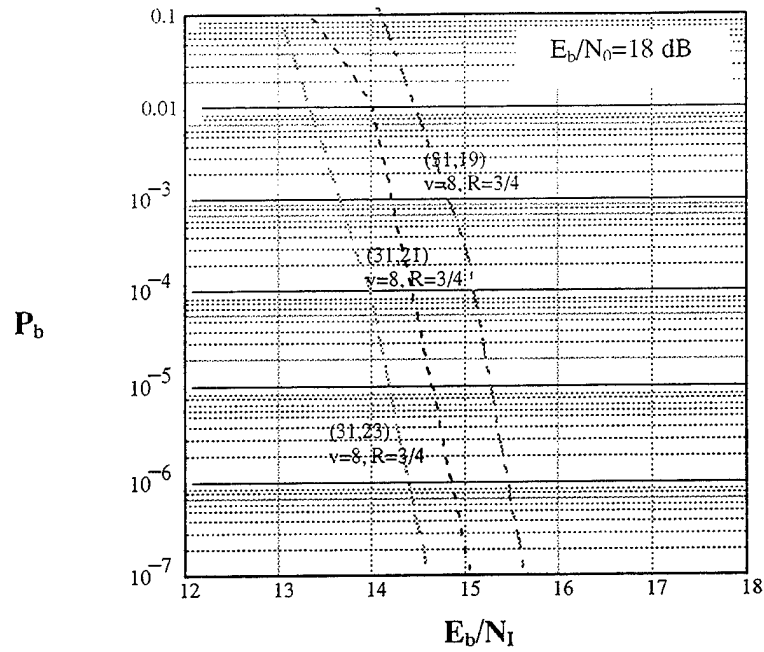


Figure 34. Performance of a fast frequency-hopped BFSK receiver with self-normalization combining in a Ricean fading channel ($a^2/2\sigma^2=10$) with concatenated coding, diversity $L=4$, and broadband interference.

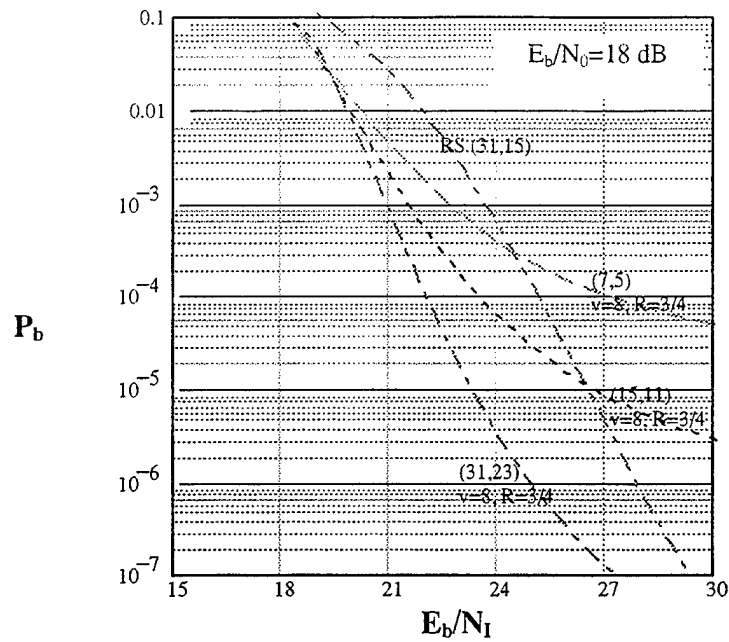


Figure 35. Performance comparison of concatenated coding and (31,15) Reed-Solomon code for a fast frequency-hopped BFSK receiver with self-normalization combining in a Rayleigh fading channel ($a^2/2\sigma^2=0$) with diversity $L=4$, and broadband interference.

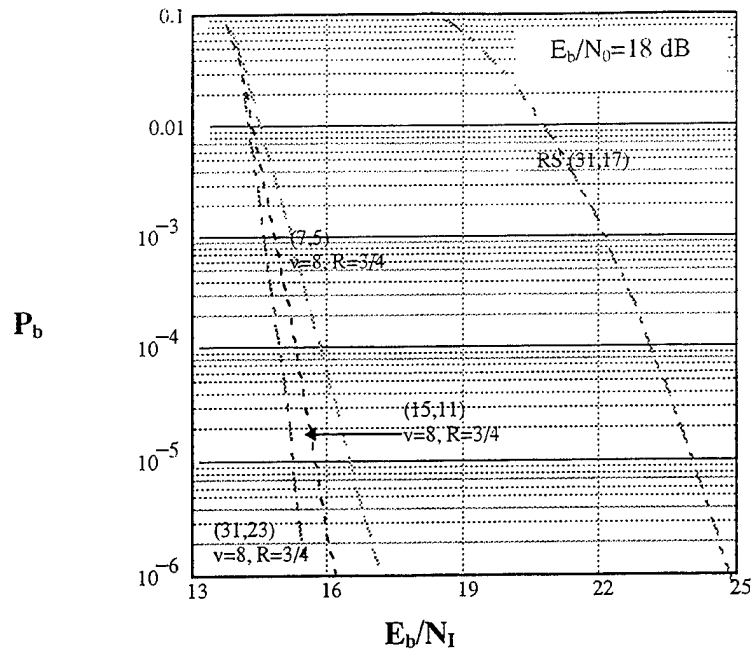


Figure 36. Performance comparison of concatenated coding and (31,17) Reed-Solomon coding for a fast frequency-hopped BFSK receiver with self-normalization combining in a Ricean fading channel ($a^2/2\sigma^2=5$) with diversity $L=4$, and broadband interference.

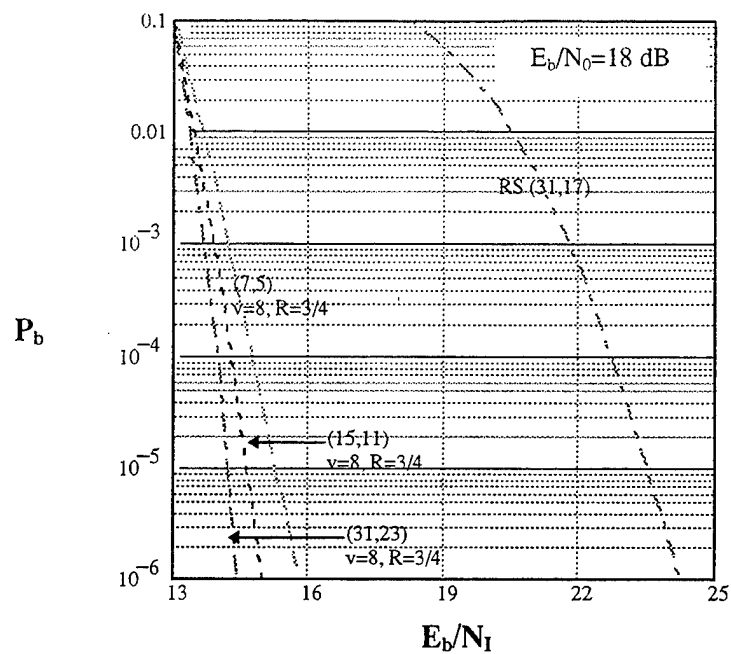


Figure 37. Performance comparison of concatenated coding and (31,17) Reed-Solomon coding for a fast frequency-hopped BFSK receiver with self-normalization combining in a Ricean fading channel ($a^2/2\sigma^2=10$) with diversity $L=4$, and broadband interference.

REFERENCES

1. B. Sklar, *Digital Communications Fundamentals and Applications*, Englewood Cliffs, NJ: Prentice Hall Inc., 1988.
2. J.G. Proakis, *Digital Communications*, 3rd ed., New York, NY: McGraw-Hill, 1995.
3. A.J. Viterbi, *CDMA Principles of Spread Spectrum Communication*, Reading, MA: Addison-Wesley Publishing Company, 1995.
4. M.K. Simon, J.K. Omura, R.A. Scholtz, and B.K. Levitt, *Spread Spectrum Communications Handbook*, New York, NY: McGraw-Hill, 1994.
5. R.L. Peterson, R.E. Ziemer, and D.E. Borth, *Introduction to Spread Spectrum Communications*, Englewood Cliffs, NJ: Prentice Hall Inc., 1995.
6. Clark and J.B. Cain, *Error-Correction Coding for Digital Communications*, New York, NY: Plenum Press, 1981.
7. G.D. Forney, Jr., "The Viterbi Algorithm", *IEEE Proc.*, vol. 61, pp. 268-278, Mar. 1973.
8. J.P. Odenwalder, *Optimal decoding of convolutional codes*, Ph.D. dissertation, School of Engineering and Applied Science, UCLA, 1971.
9. R.C. Robertson and T.T. Ha, "Error probabilities of fast-frequency hopped FSK with self-normalization combining in a fading channel with partial band interference", in *IEEE J. Select. Areas in Commun.*, vol. 10, no. 4, pp. 714-722, May 1992.
10. R.C. Robertson and K.Y. Lee, "Performance of fast-frequency hopped MFSK receivers with linear and self-normalization combining in a Rician fading channel with partial band interference", in *IEEE J. Select. Areas in Commun.*, vol. 10, no. 4, pp. 731-741, May 1992.
11. S.B. Wicker and V.K. Bhargava, *Reed-Solomon Codes and their Applications*, New York, NY: IEEE Press, 1994.
12. R.A. Khalona, "Optimum Reed-Solomon codes for M-ary FSK modulation with hard decision decoding in Rician fading channels", in *IEEE Trans. in Commun.*, vol. 44, no. 4, pp. 409-412, Apr. 1996.

13. S. Lin and D.J., Costello, Jr., *Error Control Coding: Fundamentals and Applications*, Englewood Cliffs, NJ: Prentice Hall Inc., 1983.

INITIAL DISTRIBUTION LIST

1. Defense Technical Information Center 2
8725 John J. Kingman Rd., Ste 0944
Ft. Belvoir, VA 22060-6218

2. Dudley Knox Library 2
Naval Postgraduate School
411 Dyer Rd.
Monterey, CA 93943-5101

3. Chairman, Code EC 1
Department of Electrical and Computer Engineering
Naval Postgraduate School
Monterey, CA 93943-5101

4. Prof. Tri T. Ha, Code EC/Ha 1
Department of Electrical and Computer Engineering
Naval Postgraduate School
Monterey, CA 93943-5101

5. Prof. R. Clark Robertson, EC/Rc 1
Department of Electrical and Computer Engineering
Naval Postgraduate School
Monterey, CA 93943-5101

6. Lt. Xenofon Nikolakopoulos 2
Psihari 11
Athens 11141
GREECE